Single-phase heat transfer in microchannels The importance of scaling effects

P. Rosa, T.G. Karayiannis, M.W. Collins

Accepted Manuscript

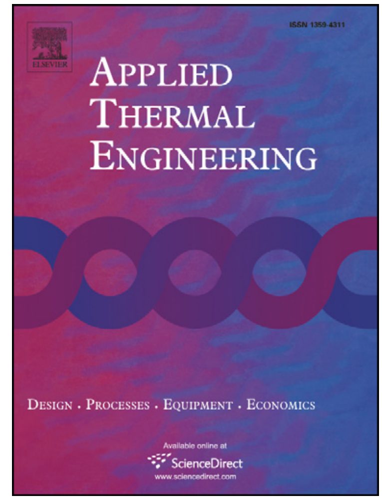

Single-phase heat transfer in microchannels The importance of scaling effects

P. Rosa, T.G. Karayiannis, M.W. Collins

PII: S1359-4311(09)00166-5
DOI: 10.1016/j.applthermaleng.2009.05.015
Reference: ATE 2817

To appear in: *Applied Thermal Engineering*

Received Date: 14 November 2008
Revised Date: 12 May 2009
Accepted Date: 16 May 2009

Please cite this article as: P. Rosa, T.G. Karayiannis, M.W. Collins, Single-phase heat transfer in microchannels The importance of scaling effects, *Applied Thermal Engineering* (2009), doi: 10.1016/j.applthermaleng.2009.05.015

Single-phase heat transfer in microchannels

The importance of scaling effects

P. Rosa[a, *], T. G. Karayiannis[b] and M. W. Collins[b]

[a] Dipartimento di Ingegneria Meccanica, Energetica e Gestionale – Università dell'Aquila
Loc. Monteluco, 67100 Roio Poggio, L'Aquila – Italy

[b] School of Engineering and Design – Brunel University West London
Uxbridge, Middlesex, UB8 3PH – United Kingdom

Abstract

Microscale single-phase heat transfer is widely used in industrial and scientific applications and for this reason, many related papers have been published in the last two decades. Nevertheless, inconsistencies between published results still exist and there is no generally accepted model for the prediction of single-phase heat transfer in microchannels. This paper presents a review of the experimental and numerical results available in the open literature. Heat transfer in microchannels can be suitably described by standard theory and correlations, but scaling effects (entrance effects, conjugate heat transfer, viscous heating, electric double layer (EDL) effects, temperature dependent properties, surface roughness, rarefaction and compressibility effects), often negligible in macro-channels, may now have a significant influence and have to be accounted for. Furthermore, measurement uncertainties may be more important, due to the reduced characteristic dimensions, so have to be accurately checked and, where possible, reduced. Experiments with single channels are more accurate and in good agreement with predictions from published correlations, in contrast to multi-(parallel) channel experiments. The latter are subject to maldistribution, 3D conjugate heat transfer effects and larger measurement uncertainties. Sub-continuum mathematical models for fluid dynamics are briefly reviewed and explained. These models are expected to gain a growing interest in the near future due to the rapid descent of microchannel dimensions down to the nano-scale. The paper concludes with a concise set of recommendations for purposes of performance and design. For single channels, available correlations for macro-channels can also give reliable predictions at the micro-scale, but only if all the scaling effects can be considered negligible. Otherwise, when scaling effects cannot be neglected or for the case of heat exchangers with parallel channels, suitable numerical simulations may be the sole alternative to carefully designed experiments to evaluate the heat transfer rates.

Keywords

Microchannels, scaling effects, measurement uncertainties, sub-continuum effects.

---

[*] Corresponding author. Tel/Fax: +39 339 6638296 E-mail: paolo.rosa78@gmail.com

Nomenclature

a	speed of sound	m/s
A	cross section area	m^2
c_p	specific heat at constant pressure	J/kgK
c_v	specific heat at constant volume	J/kgK
$d_h = 4\dfrac{A}{\Gamma}$	hydraulic diameter	m
$e = 1.6021 \cdot 10^{-19}$	electron charge	C
E_s	electric field due to the streaming potential	V/m
f	friction factor	-
F_{EDL}	body force due to the electric double layer	N/m^3
h	heat transfer coefficient	W/m^2K
H	height of a trapezoidal cross-section (Fig. 8)	m
H_{ch}	channel height (Fig. 12)	m
H_{w1}	height of the glass cover plate (Fig. 12)	m
H_{w2}	height of the copper layer (Fig. 12)	m
k	thermal conductivity	W/mK
$k_b = 1.38 \cdot 10^{-23}$	Boltzmann constant	m^{-1}
$K_{\lim}$	maximum allowable value for the EDL parameter	-
L	channel length	m
L_h	hydrodynamical entry length	m
L_t	thermal entry length	m
n_0	ionic number concentration	$1/m^3$
q	heat flux	W/m^2
q_L	heat transfer rate per unit length	W/m
r_s	average surface roughness	m
t	time coordinate	s
T	temperature	K
T_c	temperature of the heated copper surface (Fig. 12)	K
u	velocity	m/s
W_b	bottom base of a trapezoidal cross section (Fig. 8)	m
W_{ch}	channel width (Fig. 12)	m
W_t	top base of a trapezoidal cross section (Fig. 8)	m
W_w	wall width (Fig. 12)	m
x	axial coordinate	m
$X = \dfrac{x}{d_h RePr}$	dimensionless axial coordinate	-
y	transverse coordinate	m
z	valence of the positive/negative ions	-

Dimensionless groups

Br	Brinkmann number (eq. 12-13)	-
$Gz = \dfrac{RePrd_h}{L}$	Graetz number	-
$K = \kappa d_h$	EDL parameter	-
$Kn = \dfrac{\lambda}{d_h}$	Knudsen number	-
$M = \dfrac{k_w}{k_f}\dfrac{A_w}{A_f}\dfrac{1}{RePr}$	Maranzana number	-
$Ma = \dfrac{u_f}{a}$	Mach number	-

$Nu = \frac{hd_h}{k_f}$	Nusselt number	-
$Pe=RePr$	Peclet number	-
$Po=fRe$	Poiseuille number	-
$Pr = \frac{c_p \mu}{k}$	Prandtl number	-
$Re = \frac{\rho u d_h}{\mu}$	Reynolds number	-

Greek symbols

$\alpha = H_{ch}/ W_{ch}$	aspect ratio	
$\beta = \beta_T / \beta_v$		
$\beta_T = \frac{2-\sigma_T}{\sigma_T} \frac{2\gamma}{\gamma+1} \frac{1}{Pr}$	coefficient for the “temperature jump” boundary condition	
$\beta_v = \frac{2-\sigma_v}{\sigma_v}$	coefficient for the “slip flow” boundary condition	
$\gamma = c_p / c_v$	ratio between the specific heat at constant pressure and at constant volume	-
Γ	wetted perimeter	m
ε	relative permittivity of the medium	-
$\varepsilon_0 = 8.8542 \cdot 10^{-12}$	permittivity of vacuum	F/m
ϕ	dissipation function (eq. 11)	W/m^3
κ	Debye-Huckel parameter	1/m
λ	mean free path of fluid molecules	m
μ	dynamic viscosity	kg/m·s
ρ	density	kg/m^3
ρ_{el}	electric density	C/m^3
σ_v	tangential momentum accommodation coefficient	-
σ_T	temperature accommodation coefficient	-
$\xi_{\lim}$	maximum allowable ratio between the temperature rise due to viscosity and the temperature rise due to the supplied heat flux at the wall	-

Subscripts

cp	constant-properties case
f	fluid
gas	gas
in	inlet
m	mean
loc	local
out	outlet
pr	predicted
w	wall

1. Introduction

In recent years research in the field of thermofluids at the microscale level has been constantly increasing, due to the rapid growth in technological applications which require high rates of heat transfer in relatively small spaces and volumes. Recent advances in micro-electromechanical systems (MEMS) and advanced very large-scale integration (VLSI) technologies with their associated micro-miniaturization, have led to significant increases in the packing densities and heat fluxes (up to 150-200 W/cm^2) generated within these devices. In 1988, the Intel 386 processor had a power of approximately 1 W and a heat flux of approximately 0.3 W/cm^2, and sufficient cooling was possible with natural convection over the surface of the chips [1]. In 2004, the Pentium 4 dissipated 100 W, with a heat flux of around 30 W/cm^2 [2]. In 2009, according to the International Technology Roadmap for Semiconductors (ITRS), these chips are expected to have an average heat flux of 64 W/cm^2 with the maximum junction temperature requirement of nearly 90 °C [3]. As a result, many thermal engineers are confronted with an emerging task: how to find a way to solve the current or future problems of the dissipation of heat flux in electronic components. The development of new methodologies is needed by which these higher heat fluxes can be removed from silicon-based devices. The microchannel exchanger is just one of the methods that have been developed to meet such requirements.

Heat transfer in microchannels has been studied extensively during the last two decades, mainly as a result of the above search for efficient methods to cool electronic devices. Since the pioneering work of Tuckerman and Pease [4] in 1981, microchannels have revealed their capabilities for removing high heat fluxes in very compact exchangers. Along with being compact in size, microchannel heat sinks have the added benefit of providing high heat transfer coefficients. This performance is based on the premise that the heat transfer coefficient can be inversely proportional to the hydraulic diameter of the channel.

Microchannel heat sinks have been widely used for electronics cooling. The heat generated by electrical dissipation from electronic devices (e.g. microchips, MEMS, printed boards, laser diode arrays) requires very efficient cooling methods in order to maintain the temperatures at an acceptable level. For example, to avoid permanent damage to a laptop CPU, its temperature should not exceed 80-90°C. Both the performance reliability and life expectancy of electronic equipment are inversely related to the temperature of the components of the equipment. Therefore, reliable performance and long life may be achieved by effectively controlling the operating temperature. *The concept of the microchannel, fabricated as an integral part of silicon based devices, combines the positive attributes of high compatibility with electronic chips, high ratio of surface area per unit volume and high potential heat transfer performance, together with highly sophisticated and economically competitive fabrication processes.* Therefore, thermal management is, and will continue to be, one of the most critical areas in electronic products development. It will have a significant impact on the cost, overall design, reliability and performance of the next generation of microelectronic devices.

In the last few years, several other applications have been proposed for micro-heat sinks. Recent fields of application are in the automotive, chemical and food industries, environmental technology, and the aviation and space industries [5]. Examples include: Brandner et al.'s [6] proposal for an electrically powered micro-heat exchanger (around 1 cm^3 active volume with the number of rectangular channels and the hydraulic diameter ranging from 650 to 2279 and from 144 to 70 *μm*, respectively) for use in the production of biodiesel fuel; the Printed Circuit Heat Exchanger (PCHE), whose channels can have hydraulic diameters less than 2 *mm*, is widely used in petrochemical plants and fuel cells [7]; Martin et al.'s [8] design for a heat exchanger for a micro heat pump, for heat loads of 100 W/cm^2. The latter was made of over 150 square microchannels whose side was 100 *μm*. Finally, compactness and lightness of weight have turned the interest of the car industry towards mini- and micro-heat exchangers, and it is possible to find heat exchangers in this industry with hydraulic diameters around 1 mm [9].

An increasingly large volume of research work in micro-scale heat transfer has been recently reported in the literature. Despite the growing number of realized applications of microchannels in science and engineering, there is still a low level of understanding of the relevant fluid dynamics and heat transfer processes. The published results often disagree with each other and with heat transfer correlations for large sized channels. Some authors claim that new phenomena occur in microchannels, while many others report that several effects usually neglected in standard correlations (effects of surface roughness, fluid viscosity, temperature dependent properties, conjugate heat transfer between fluid and solid walls) can become relevant in microchannels. Whatever the heat transfer processes in microchannels actually are, they have to be suitably understood to achieve a successful design of the heat sinks .

First of all, it is necessary to define the term microchannels. As they are understood to be different from large-sized ones, a possible definition is channels with a hydraulic diameter below a threshold for which significant discrepancies arise, with respect to "normal" channels, in fluid dynamics and heat transfer behaviour. For example, Adams et al. [10] found 1.2 *mm* for the hydraulic diameter as the lower limit for the applicability of standard turbulent single-phase Nusselt-type correlations to non-circular channels. However, there is no agreement in the literature whether such differences exist, and if they do, at what length scales they become relevant. *In the present paper, following Celata [9], a geometrical and straightforward definition of microchannel will be used: a microchannel is defined as a channel whose hydraulic diameter lies between 1 μm and 1 mm.*

One cause of the above discrepancies is surely in the difficulty of performing reliable measurements in microdevices. Hence, the related uncertainty could be quite high, sometimes explaining the deviations with respect to the standard results. In fact, Guo and Li [11] reported that in their experiments on flow resistance in a circular glass tube, they initially measured the diameter as 84.7 *μm* using a 40x microscope. The data reduction with this measured diameter showed that the friction factors were larger than that predicted by conventional theory. The average value of the diameter measured using a 400x microscope for the same microtube was only 80.0 *μm*. With this more accurate value of the diameter, the friction factors obtained from the experimental data were in good agreement with the conventional values ($f \cdot \mathrm{Re}=64$). Morini [12], from a chronological analysis of published experimental results, has noted that the deviations between the behaviour of fluids through microchannels with respect to large-sized channels are decreasing as time progresses. This could be explained by improvements in fabrication and measurement techniques. As a consequence, he questioned the applicability of older results for comparison purposes.

However, measurement uncertainties cannot always explain all the reported discrepancies. When the length scales reduce to the micron range, several physical phenomena, usually neglected in macrochannels, may have a sensible influence on fluid flow and heat transfer.

2. SCALING EFFECTS IN MICROCHANNELS

Heat transfer in large-sized channels has been extensively analyzed during the last two centuries and its theory and results can now be considered well-established with accepted correlations. For example, for fully developed laminar flow, the Nusselt number Nu is a constant whose value depends only on cross-sectional geometry and boundary conditions. For circular tubes, Nu = 3.66 and Nu = 4.36 for isothermal tube surface and constant heat flux boundary conditions, respectively. Experimental analyses confirmed that, for a long tube where the entrance effects can be ignored, the average Nusselt number, based on the logarithmic mean temperature difference between the tube wall and the fluid, tends towards the reported values. The above results are obtained under the following assumptions:

1. steady fully developed flow;
2. the thermophysical properties of the fluid do not vary with the temperature;
3. the fluid can be treated as a continuum medium;
4. incompressible flow;
5. simplified boundary conditions (constant wall temperature or constant wall heat flux);
6. the heating due to viscous dissipation can be neglected;
7. surface roughness has negligible effects (for laminar flows).

In microchannels, depending on whether the flow is liquid or gaseous, several of the above assumptions may no longer be made. Hence, the so-called "scaling effects" [13] have to be considered. Being compact in size and capable of transferring high heat transfer rates, flows in microchannels may be subjected to high temperature variations and the entry region may cover a significant fraction of the whole channel length. Hence, assumptions 1 and 2 may not be valid and *entrance effects* and *temperature-dependent property effects* on the heat transfer may be significant. For gas flows, but not liquids, assumptions 3 and 4 become questionable. Due to the low values of the hydraulic diameter, down to few μm, the molecular free path of the fluid can be non-negligible with reference to the hydraulic diameter, leading to significant *rarefaction effects*. Slip flow and temperature jump at the wall should be accounted for and, at increasing rarefaction, the fluid may be no longer modelled as a continuum and mathematically mesoscopic or microscopic models should be used (Section 4). Furthermore, the pressure drop in microchannels can be quite large and the compressibility of the gas may play a significant role in the heat transfer (*compressibility effects*). Established correlations available in the open literature for the evaluation of the Nusselt number in flows inside channels are obtained for prescribed boundary conditions of constant wall temperature (CWT) or constant wall heat flux (CWHF). However, in microchannels, heat conduction in the fluid and the solid walls, neglected in large channels, may strongly modify the heat transfer pattern at the boundaries. Therefore, *conjugate heat transfer effects* should be taken into account. Due to the reduced length scale, the surface-to-volume ratio increases in microchannels. As a consequence, all of the phenomena confined in the zone of interaction between the flow and the solid walls gain relevance. Then, *viscous heating effects* and *surface roughness effects* on heat transfer have to be checked. Moreover, for liquid flows made by aqueous solutions, *electric double layer* (EDL) *effects*, due to the interaction between the electrostatic charges on the solid surfaces and the ions in the solution, may influence the heat transfer and should be accounted for. Finally, it has to be remembered that the Nusselt number, also for fully developed flows, *depends on the cross-sectional geometry*. For example, for CWT, Nu = 3.66 and Nu = 2.98 for circular and square cross sections, respectively. Furthermore, for rectangular cross sections, the Nusselt number depends also on the aspect ratio α (i.e. the ratio between the smaller to the larger side), increasing from 2.98 for $\alpha = 1$ (square channel) to 7.54 for $\alpha = 0$ (deep rectangular channels). It is worth stating that, for the comparisons between experimental results and correlations to be meaningful, *the cross sections must be the same*.

Over the past 20-25 years, despite the publication of a very large number of dedicated papers, inconsistencies between the results still exist. Several reviews have attempted to draw some overall conclusions and to recommend the direction of new researches. A number of these reviews, all in the last few years, will be assessed.

Hetsroni et al. [14] observed that, when comparing the experimental published data with simple 1D models that assume, for example, constant thermophysical properties, constant heat transfer coefficients and uniform wall temperature or heat flux, there are significant discrepancies between the measurements and the theoretical predictions and some “new effects” are often called for to adjust the models and make them match the experiments. On the other hand, numerical solutions based on the Navier-Stokes and energy equations but taking account of the “proper” boundary conditions (such as varying thermophysical properties, conjugate heat transfer between the fluid and the solid walls) demonstrated a fairly good agreement with available experimental data. The authors generalized the results as follows:

- the effect of viscous dissipation is negligible under typical flow conditions;
- at low Reynolds numbers (Re < 150) axial heat conduction in the fluid and the wall can affect significantly the heat transfer and decrease the Nusselt number;
- any experimental results based only on measurements of fluid temperature at the inlet and the outlet manifolds of the heat sink may lead to incorrect values of the Nusselt number;
- the heat transfer coefficient depends on the characteristics of the wall temperature and the bulk fluid temperature variation along the heated tube wall. It is well known that under certain conditions the use of mean wall and fluid temperatures to calculate the heat transfer coefficient may lead to peculiar behaviour of the Nusselt number;
- accurate estimation of the heat transferred through the solid substrate in experiments should be achieved;

- the experimental heat transfer coefficient calculated numerically, using the exact model with regard to the heat transferred through the solid substrate, represents the correct variation of the Nusselt number with respect to the Reynolds number;
- the thermal entry length should be considered when comparing experimental and numerical results.

Obot [15] reviewed many published experimental results about microchannels and found that:

- for heat transfer in the laminar regime the macro-scale behaviour is such that the ratio $Nu/Re^{0.5}Pr^{0.4}$ is approximately constant, for hydraulic diameters between 150 and 1000 μm. Analyzing several published results which seemed to have significant discrepancies with respect to conventional predictions, the ratio $Nu/Re^{0.5}Pr^{0.4}$ was approximately the same for all of them, even if with a large scatter (up to 25%). Notwithstanding, given the experimental uncertainties in measured *Nu*, the error bands on the correlation, and the working fluid, data deviations from well-established relationships of the order of 25% could be very well expected and should be considered satisfactory.

Based on the above findings, Obot concluded that satisfactory estimates of heat transfer coefficients for microchannels, within the accuracy of the experimental error, can be obtained by using either verifiable experimental data for channels of large hydraulic diameters or conventional correlations.

Palm [16] reviewed several works about single-phase heat transfer in microchannels and found that there is no general agreement about the threshold diameter below which classical fluid-dynamics and heat transfer theories seem no longer to be applicable. He observed that both higher and lower friction factors and Nusselt numbers have been reported, and reviewed several reasons that have been proposed to justify these discrepancies: surface roughness effects, entrance effects, EDL effects, non-constant fluid properties, two- and three-dimensional transport effects, and slip flow (for gases only). Moreover, since the pressure drop is inversely proportional to the fourth power of the hydraulic diameter and the heat transfer coefficient is related to the logarithmic mean temperature difference between the fluid and the wall, and due to the difficulties in accurately determining these parameters, the large scatter in the results is partly attributable to experimental uncertainties.

Rostami et al. [17] focused on published results for gas flows in microchannels and highlighted the inability of rarefaction effects to always account for the discrepancies in the experimental results. These could sometimes be due to measurement inaccuracies, roughness effects, unidentified blockages in the channels, unaccounted heat losses, and pressure non-linearities along the channel. Their overall recommendation was that more experiments were needed to achieve a better general understanding of fluid flow and heat transfer phenomena at the micro-scale.

Morini [12] reviewed 90 papers about fluid flow and heat transfer in microchannels. Regarding heat transfer, he observed that:

- there is a very large scatter in published results;

- several scaling effects (surface roughness effects, EDL effects, rarefaction and compressibility effects, variable thermophysical properties, viscous heating, electro-osmotic phenomena) can have a significant influence at the micro-scale.
- the Nusselt number has been found to be both increasing and decreasing with the Reynolds number in the laminar regime;
- several heat transfer correlations for microchannels have been proposed, which seem to predict well only their own experimental points;

Finally, he highlighted the fact that the deviations between the behaviour of fluids through microchannels with respect to the large-sized channels are decreasing. As mentioned earlier, this is probably due to the increased reliability/accuracy of the more recent published data and to the great improvement of microfabrication techniques, with a more precise control of the channel cross-sections and surface roughness. Hence, data from older studies may not provide reliable information.

All of the reviews mentioned above are consistent with the following statements:

- there are no new effects in microchannels, but phenomena usually neglected in macro-channels (*scaling effects*) have now a relevant influence on the heat transfer;
- the test rigs have to be designed in such a way that all the heat losses are negligible with respect to the heat flux from the wall to the fluid, so as to really achieve the supposed boundary condition (constant wall temperature or constant wall heat flux), and for the measurements to provide really reliable final data;
- when the scaling effects are properly taken into account, the classical fluid dynamics theory and correlations seem to be in reasonable agreement with the experimental data.

In the following, the scaling effects for microchannels will be studied in detail and the most recently published results reviewed. Since most of the examined papers study the influence of several scaling effects, they may be cited several times in our overall treatment, once for each scaling effect they analyzed.

2.1 Entrance Effects (EE)

The Nusselt number for laminar flows in a channel is constant only for fully developed flows, i.e. when both the velocity and the temperature profile remain unchanged. In the entrance region, the velocity and temperature profiles are developing and the Nusselt number varies. In classical fluid-dynamics theory, two entry lengths are usually defined:

- hydrodynamical entry length, L_h, after which the velocity profile is fully developed;
- thermal entry length, L_t, after which the temperature profile is fully developed.

When both the velocity and the temperature profile developing lengths have a significant influence on the Nusselt number, the flows are said to be *simultaneously developing* (SD), i.e. they are both hydrodynamically and thermally developing flows. When the velocity profile can be considered fully developed and only the thermal entry length effects need to be considered, the flows are termed *thermally developing* (TD), which is the most typical situation for flows with $Pr > 1$ (for example, $Pr \approx 5.5$ for water at 20 °C). Correlations both for the local and the average Nusselt number exist in the specialized literature both for SD and TD flows, and for different cross-sectional geometries. Some of them will be introduced and compared in Section 3.

Entrance effects have of course always to be accounted for when calculating the local Nusselt number. The average Nusselt number, on the other hand, is a constant for fully developed flows, but it has been seen to increase with the Reynolds number, when the entrance effects have a significant influence. The Graetz number is defined as in eq. (1) and is used as a criterion for neglecting the entrance effects.

$$Gz = \frac{RePrd_h}{L} \tag{1}$$

Morini [18] stated that the entrance effects on the average Nusselt number can be neglected if the following inequality is satisfied:

$$Gz < 10 \tag{2}$$

Compactness is one of the most important characteristics of microchannel heat sinks and their length L can be small. Then, according to eq. (1)-(2), entrance effects may be relevant at moderate or high Reynolds numbers and have to be considered. Fig. 1 shows, for a water flow (Pr = 5.5), the channel length L above which entrance effects may be neglected, as a function of the Reynolds number, with the hydraulic diameter as a parameter. L easily exceeds 50 *mm* for $Re > 500$, except for d_h = 0.1 *mm*, meaning that entrance effects, for the most typical microchannel dimensions, have always to be considered and often to be accounted for.

Lee et al. [19] investigated heat transfer in rectangular microchannels of different hydraulic diameters (318-903 μm), for Re = 300-3500, using deionized water. The heat sink was made of copper with ten machined parallel microchannels. Using a standard commercial numerical thermofluids code, they also formulated a model for the 3D conjugate heat transfer in the microchannel heat sink, accounting for both convection in the channel and conduction in the substrate. They simulated both TD and SD laminar flows. They also developed simplified models by assuming less complex boundary conditions around the microchannel flow domain and proposed the use of the “thin wall” model (axially uniform heat flux with circumferentially uniform temperature boundary condition). The Nusselt number, based on the difference between the measured mean channel walls and fluid temperatures, was found to increase with the Reynolds number. However, it was in disagreement with all the tested correlations for heat transfer in developing flows. On the other hand, they found good agreement between their experimental results and their numerical predictions, thanks to the better matching of boundary conditions and entrance effects with those of the real flow. For these reasons, they suggested employing numerical simulations to predict the heat transfer behaviour of microchannels, instead of using correlations.

Gao et al. [20] studied conduction and entrance effects in deep rectangular microchannels, with Reynolds numbers in the range 200-3000, hydraulic diameters between 0.2 and 2 mm, and using water as the test fluid. They observed good agreement of the measured Nu and the correlation of Shah and London [21] for hydraulic diameters down to 1 mm, while significant reductions were observed for lower values.

Morini [18], considering a 2D steady laminar fully developed flow with constant thermophysical properties, analysed the influence of several scaling effects (viscous heating, conjugate heat transfer and entrance effects) on the Nusselt number. With reference to the entrance effects, his highlighted conclusion was that, as previously stated, they could be significant at moderate or high Reynolds number.

Using a single, stainless steel, microtube, Bucci et al. [22] determined Nusselt number for degassed and demineralised water, with the Reynolds number ranging from 200 to 6000, for constant wall temperature. Three tube diameters were tested (172, 290 and 520 μm). In the laminar flow regime, the Nusselt number increases with Reynolds number as in TD flows, but deviates from the Hausen correlation [23] (see section 3). The largest microtube shows an increase in Nusselt number to up to 17% higher than the predicted one, whilst the smallest one deviates by up to 55% higher than the predicted value.

Celata et al. [24] analyzed single-phase heat transfer for water flows in single microtubes with diameters ranging from 528 down to 50 μm and *Re* ranging from 600 to 4500. The tested microchannel was mounted inside a vacuum capsule to avoid convective heat losses to the surroundings; the heat losses due to radiation, to axial conduction in the walls and to viscous heating were estimated to be negligible as well. The local laminar Nusselt number was found to depend on the axial position, due to thermal entrance length effects, and on the local Reynolds number. Decreasing the channel diameter led to a lower Nusselt number and weakened its dependence on the Reynolds number and the axial position. Similarly, the average Nusselt number demonstrated a slight dependence on the Reynolds number and decreased with reducing channel diameter. For larger diameters, this behaviour could be due to the thermally developing flow. For smaller diameters, however, the conduction heat losses in wires for example, became probably quite significant with respect to the convective heat transfer in the flow, because of the small flow rates probably influencing the measurements. In fact, experimental results for the Nusselt number agreed reasonably with the Hausen correlation [23] (see section 3) for TD flows with constant wall heat flux for diameter down to 325 μm; for smaller diameters, the agreement deteriorates due to measurement uncertainties.

Liquid crystal thermography was proposed by Muwanga and Hassan [25] for local heat transfer measurements in microchannels. They found that the Nusselt number for deionized water flow in a 1 mm diameter microtube with constant heat transfer wall flux was in good agreement with the analytical solution for thermally developing flows in the laminar regime [21].

Lelea et al. [26] studied experimentally heat transfer and fluid flow for distilled water in the laminar regime. They used single circular microchannels with 125.4, 300 and 500 μm hydraulic diameter and found good agreement between the measured Nusselt numbers, their numerical predictions and the analytical results (Nu = 4.36, for fully developed laminar flows) as well as with the Shah and London [21] theoretical values for thermally developing laminar flows.

The Graetz numbers for some of the experimental papers just examined are reported in Table 1. Since they always exceed 10, the results obtained in the papers must only be compared with correlations which are able to account for entrance effects. *It can also be concluded that, for heat transfer in microchannels, entrance effects have always to be taken into account.*

2.2 Temperature dependent properties

The difference in fluid temperature between the inlet and the outlet could be high in microchannels, also accentuated by viscous heating effects. Hence, the variation of the thermophysical properties along the channel could sometimes explain the apparent deviations of the microchannel flow and heat transfer [27]. Herwig and Mahulikar [28] evaluated the influence of the temperature dependence of the thermophysical properties. Performing an order of magnitude analysis on a thermally and hydrodynamically fully developed flow in a microtube, they showed that the axial fluid temperature gradient is of the order of $1/d_h$ and, while negligible in large channels, can be very high at the microscales. The difference ΔNu_{cp} between the actual Nusselt number, Nu, and that for the constant property case, Nu_{cp}, divided by Nu_{cp} i.e.

$$\Delta Nu_{cp} = \frac{Nu - Nu_{cp}}{Nu_{cp}} \tag{3}$$

can be obtained from the results depicted in Fig. 2, for water flow at Re = 75 and inlet temperature T_{in} = 50 °C. It can be seen that the effect on the Nusselt number due to the variation of the thermophysical properties is up to +5.65% for a heat flux per unit surface area $q_w = +30$ W/cm^2 (i.e. the fluid is heated) and up to -9.62% for $q_w = -30$ W/cm^2 (i.e. the fluid is cooled). Hence, they can be significant and should be checked.

2.3 Rarefaction effects

As mentioned above, rarefaction effects are significant only for gas flows. The standard expressions of the continuity, Navier-Stokes and energy equations rely on the assumption that the fluid may be treated as a continuum. For this assumption to be fulfilled, the mean free path, λ, of the fluid molecules, has to be much lower than a characteristic length scale of the system. The Knudsen number, $Kn = \lambda / d_h$, is usually used to check whether the fluid can be considered a continuum and, hence, if the Navier-Stokes equations can still apply. Gad-el-Hak [29] proposed the following criteria:

1. $Kn \le 10^{-3}$: no-slip flow;
2. $10^{-3} \le Kn \le 10^{-1}$: slip flow;
3. $10^{-1} \le Kn \le 10$: transition flow;
4. $Kn > 10$: free-molecule flow

In regime 1, the fluid can be considered a continuum and the usual boundary condition of no-slip velocity and no-temperature jump at the wall apply. In regime 2, the continuum assumption is still valid; hence the Navier-Stokes equations can still be employed, but slip flow and temperature jump at the solid boundaries have to be considered. Von Smoluchowski [30] developed, for gas flow with isothermal walls, the following expressions for the slip flow and the temperature jump at the wall respectively:

$$u_{gas} - u_w = \frac{2-\sigma_v}{\sigma_v} \lambda \left.\frac{\partial u_{gas}}{\partial y}\right|_w + \frac{3}{4} \frac{\mu_{gas}}{\rho_{gas} T_{gas}} \left.\frac{\partial T_{gas}}{\partial x}\right|_w \quad \text{(slip flow at the wall)} \tag{4}$$

$$T_{gas} - T_w = \frac{2-\sigma_T}{\sigma_T} \frac{2\gamma}{\gamma+1} \frac{\lambda}{Pr} \left.\frac{\partial T_{gas}}{\partial y}\right|_w \quad \text{(temperature jump at the wall).} \tag{5}$$

σ_v and σ_T are the tangential momentum and temperature accommodation coefficients, respectively. For real walls, some molecules reflect diffusively and some reflect specularly. σ_v and σ_T can be considered as the fraction of the incoming tangential momentum and energy flux reflected diffusively during the interaction of the fluid molecules with the solid walls.

Neglecting thermal creep effects, represented by the term $\frac{3}{4} \frac{\mu_{gas}}{\rho_{gas} T_{gas}} \left.\frac{\partial T_{gas}}{\partial x}\right|_w$ in eq. (4), eq. (4) and (5) are often written as:

$$u_{gas} - u_w = \beta_v \lambda \left.\frac{\partial u_{gas}}{\partial y}\right|_w \tag{6}$$

$$T_{gas} - T_w = \beta_T \lambda \left.\frac{\partial T_{gas}}{\partial y}\right|_w \tag{7}$$

where $\beta_v = \frac{2-\sigma_v}{\sigma_v}$ and $\beta_T = \frac{2-\sigma_T}{\sigma_T} \frac{2\gamma}{\gamma+1} \frac{1}{Pr}$. If we consider, for example, air at standard pressure and temperature, its mean free path is $\lambda \cong 0.065$ μm [29]. Therefore, a microchannel with a hydraulic diameter of 10 μm would have Kn = 0.0065, which is in the slip flow regime. Velocity slip increases the local fluid velocity at the wall, thus enhancing convective heat transfer between the fluid and the wall, while a temperature jump decreases the temperature gradient at the wall and hence the heat transfer. Therefore, the rarefaction effects on heat transfer are not obvious, but depend on the relative influence of slip flow and temperature jump (i.e. on the ratio $\beta = \beta_T / \beta_v$). Fig. 3, from Ghodoossi and Egrican [31], shows the variation of the Nusselt number with β, for different values of the product $\beta_v Kn$, in a rectangular microchannel. For $\beta < 0.5$ the Nusselt number for fully developed flows increases with respect to the absence of rarefaction effects, since the increase in heat transfer due to the slip flow prevails on the reduction due to the temperature jump. Otherwise, for $\beta \geq 0.5$, temperature jump effects prevail over those of the slip flow and the Nusselt number decrease. β_T / β_v =1.667 is often proposed as a typical value for engineering applications with air [32]; in this case, rarefaction effects tend to reduce Nusselt number. In regimes 3 and 4, for transition and free-molecular flows respectively, the continuum assumption breaks down. The Navier-Stokes equations are no longer applicable and molecular effects have to be addressed [33]. These important situations will be discussed in Section 4, but it should be noted here that "transition" refers to molecular significance, and not to the laminar/turbulent transition.

The problem of hydrodynamically fully developed and thermally developing laminar slip flow in a microchannel formed by two parallel plates, with uniform wall temperature boundary condition, was successfully addressed by Mikhailov and Cotta [34] and Chen [35]. Mikhailov and Cotta [34] neglected energy viscous dissipation and considered temperature-independent thermophysical properties. They used the integral transform approach and the solution of the related eigenvalue problem in terms of hypergeometric functions. Chen [35] also accounted for viscous dissipation and solved the energy equation by means of the integral transformation techniques, considering the first 25 eigenfunctions of the solution. In comparison with the continuum condition, heat transfer may be enhanced, reduced or unaffected, depending on the competition between the effects of these parameters. For a given value of the product $\beta_v Kn$ the local Nusselt number profile becomes flatter and the thermal entrance length is shortened when β_T / β_v increases. Also, the fully developed Nusselt number decreases with increasing $\beta_v Kn$ (i.e. increasing rarefaction) for $\beta_T / \beta_v > 0.2$, and increases for $\beta_T / \beta_v = 0$ (i.e. neglecting temperature jump). For $Kn\beta_v$ = 0.1, Mikhailov and Cotta [34] obtained, for $\beta_T / \beta_v = 1$, a fully developed Nusselt number, referred to the hydraulic diameter, of 3.01[†], while Chen [35] calculated, for $\beta_T / \beta_v = 2$, a value of 3.33. Both these values are sensibly lower than the classical value of 7.54 and give an idea of the influence of rarefaction on heat transfer.

Jeong and Jeong [36] analyzed the extended Graetz problem in a flat channel (parallel plates) including effects of rarefaction, viscous dissipation and streamwise conduction altogether, assuming a thermally developing Poiseuille flow. They considered both constant wall temperature and constant wall heat flux boundary conditions. The fully developed Nusselt number decreased with increasing *Kn*. For *Kn* = 0.08 (slip flow regime) it is around 4.10, against the 7.54 classical value.

Godoossi and Eğrican [31] calculated velocity and temperature fields by an analysis of fully developed steady laminar slip flow in rectangular microchannels. The temperature boundary condition was complex: the temperature was uniform in the cross-section edges but varied linearly in the longitudinal direction. They found that the Nusselt number has a weak dependence on the wall temperature and is sensibly influenced by channel aspect ratio. Rarefaction effects on the Nusselt number depend on the combined influence of slip flow and temperature jump at the wall (Fig. 3). For a slip flow with small temperature jump ($\beta_T / \beta_v < 0.5$), *Nu* increases with increasing $Kn\beta_v$, because of enhanced

---

[†] The Nusselt number is defined by the authors as $Nu = \frac{hH_{ch}}{k_f}$, where H_{ch} is the spacing between the parallel plates, and found a value for fully developed flow equal to 1.50462. The hydraulic diameter may be calculated as $d_h = \frac{4A}{\Gamma} = \frac{4H_{ch}W_{ch}}{2(H_{ch}+W_{ch})} \approx 2H_{ch}$, for the situation where the width of the channel W_{ch} >> H_{ch}. Hence, the Nusselt diameter referred to the hydraulic diameter is $Nu = 2\frac{hH_{ch}}{k}$, i.e. two times the one defined by the authors.

convection at the wall. When the temperature jump increases ($\beta_T/\beta_v > 0.5$), the temperature gradient in the fluid reduces and so does the Nusselt number, since this effect overcomes the enhancement in convection due to slip flow. Finally, for $\beta_T/\beta_v = 1.667$, which is often proposed as a reference value for engineering applications, the Nusselt number reduction for increasing $Kn\beta_v$ is larger for deep rectangular channels than for square channels.

Cao et al. [37] performed a numerical analysis of fully developed laminar slip flow and heat transfer in trapezoidal microchannels with a uniform heat flux boundary condition, ignoring viscous dissipation. As for rectangular microchannels, the aspect ratio has a significant influence on the Nusselt number, and so does the base angle. Similarly with the findings of Godoossi and Eğrican [31], who used rectangular microchannels, *Nu* increases with $Kn\beta_v$ when $\beta_T/\beta_v < 0.5$ and decreases otherwise.

Using the integral transformation technique, Tunc and Bayazitoglu [38] studied 2D steady state, laminar, hydrodynamically developed flow in microtubes with uniform temperature and uniform heat flux boundary conditions. They accounted for slip velocity and temperature jump at the boundaries, and viscous heating in the fluid, but assumed constant fluid properties. They found the fully developed Nusselt number decreased as the Knudsen number increased, because of the temperature jump at the walls. For $\beta_T/\beta_v = 1.667$, the Nusselt number decreased from 3.68 for $Kn = 0$ to 2.54 for $Kn = 0.1$, for the boundary condition of constant wall temperature, and from 4.36 to 2.90 for constant wall heat flux. Once again, neglecting temperature jump but considering only the slip velocity led to an increase in Nusselt number with increasing *Kn*.

Myong et al. [39] analyzed the effects of slip flow and temperature jump at the walls, in a circular tube, using both the Von Smoluchowski model [30], described above, and the Langmuir model [40], where the slip model is derived taking into account the interfacial interaction between the gas molecules and the surface molecules. The fully developed Nusselt number, for a flow with constant wall temperature, was found to decrease from 3.657, for $Kn = 0$, to 3.446 (Von Smoluchowski model), and 3.355 (Langmuir model), for a rarefied flow with $Kn = 0.02$.

The following conclusions about rarefaction effects may be drawn:

- for rarefied gases ($Kn > 0.001$), slip flow and temperature jump at the wall have to be taken into account;
- slip flow at the wall tends to increase the fully developed Nusselt number, while temperature jump tends to decrease it. Hence, the Nusselt number in rarefied flows can both increase or decrease, depending on the relative importance of the above cited phenomena. When the temperature jump can be neglected (i.e. for very small values of β_T/β_v), the Nusselt number increases. However, for the most typical values of β_T/β_v in engineering applications ($\beta_T/\beta_v \approx 1.667$), rarefaction effects tend to significantly reduce the Nusselt number. For example, for slip flow in circular microchannels with constant wall temperature, the Nusselt number varies from 3.68 for Kn=0 to 2.54 for Kn=0.1;

- for rectangular and trapezoidal microchannels, the aspect ratio has a significant influence on the Nusselt number, both for standard and for rarefied flows.

2.4 Compressibility effects

Being related to density variations, compressibility effects do not affect liquid flows and may be relevant only for gas flows. When the Mach number of a gas flow is below 0.3, that flow is treated as incompressible. However, the Ma<0.3 criterion is only a necessary but not sufficient condition to allow the flow to be considered to be approximately incompressible [29]. In some microdevices, the pressure may strongly reduce along the flow direction due to viscous effects even though the speeds may not be high enough for the Mach number to exceed the traditional threshold of 0.3. The gas density would therefore vary and these variations change both the velocity and the temperature profiles, thus strongly affecting the heat transfer behaviour. Guo and Li [11] reviewed several papers about compressibility effects on fluid flow and heat transfer at microscale. They showed that the Mach number can significantly increase along the flow in microchannels, although the inlet value is quite far from the compressibility threshold. As a consequence, the velocity and temperature profiles vary continuously and hence, so does the local Nusselt number. Fig. 4.A shows the radial temperature profile at different locations along the flow. The temperature reduces in the channel interior, because of the work due to the expansion of the gas, and increases in the near-wall region because of viscous dissipation. The local Nusselt number may even be negative, Fig. 4.B, if the Mach number and the resulting temperature decrease in the channel interior are large enough. This is physically meaningless and can be attributed to an inappropriate definition of the characteristic temperature difference. The authors suggested the use of the adiabatic temperature difference, instead of the difference between the wall temperature and the bulk fluid temperature, to describe the channel heat transfer in high speed flows.

It can be concluded that

- compressibility effects have to be checked in gas flows, as they can influence significantly the flow and heat transfer.

2.5 Conjugate heat transfer

The standard correlations for heat transfer in channels are valid under the idealized CWT or CWHF boundary conditions. Moreover, they are usually obtained for fully developed flows. In micro-heat sinks, however, it is difficult to achieve such conditions, particularly with several parallel microchannels. Conduction in the solid and in the axial direction of the fluid can have a strong influence on the heat patterns (conjugate heat transfer) particularly at low Re, and should be accounted for.

Fedorov and Viskanta [41] investigated conjugate heat transfer in a heat sink with rectangular microchannels. They modeled the 3D incompressible laminar steady flow and the heat conduction in the silicon substrate. They obtained good agreement with experimental results and found very complex heat flow patterns, showing that there is a very strong coupling between convection in the fluid and conduction in the silicon substrate, that can only be resolved by a detailed 3D simulation.

The work of Lee et al. [19] has already been introduced above in Section 2.1. It is remarked here that their experimental results disagreed with all of the tested correlations but were well predicted by numerical simulations, provided a full 3D conjugate heat transfer model was used. Good agreement was also obtained when using the "thin wall model", highlighting the importance of setting accurate boundary conditions in the simulations. For this reason, the authors recommended the use of numerical simulations with suitable boundary conditions, instead of correlations, to predict the performance of heat sinks using microchannels.

Gamrat et al. [42] studied conduction and entrance effects in rectangular microchannels both experimentally and numerically, with a 3D conjugate heat transfer model, Reynolds numbers in the range 200-3000, d_h between 0.2 and 2 mm, and using water as the test fluid. They observed a significant reduction in the measured Nu when the hydraulic diameter was below 1 mm. This reduction was not predicted by their numerical model, despite its geometry being a full description of the particular experimental setup used.

Morini [18], considering a 2D steady laminar fully developed flow with constant thermophysical properties, analysed the influence of several scaling effects (viscous heating, conjugate heat transfer and entrance effects) on the Nusselt number. He suggested that the dependence of the mean Nusselt number on Reynolds number even in the laminar regime may be explained taking into account conjugate heat transfer, viscous and entrance effects. Fig. 5 shows how these scaling effects can change the average Nusselt number. At low Reynolds numbers, the heat transfer by conduction in the fluid and the solid substrate is not negligible relative to the heat transfer from the wall to the fluid and tend to reduce the Nusselt number. At moderate Reynolds numbers, entrance and viscous heating effects become relevant, and tend to increase (entrance effects) or decrease (viscous heating effects) the Nusselt number.

Maranzana et al. [43] introduced a dimensionless number M, the Maranzana number, which can be seen as the ratio between the axial heat conduction in the solid walls of the channel and the heat transfer by convection in the fluid:

$$M = \frac{k_w}{k_f} \frac{A_w}{A_f} \frac{1}{RePr} \tag{8}$$

where A_w is the cross-sectional area of the solid walls of the channel and A_f the area of the surface wetted by the flow. For the axial heat conduction in the solid walls to be neglected, Maranzana et al. proposed the following criterion:

$$M < 0.01 \tag{9}$$

As observed by Morini [18], eq. (8) shows the importance of conjugate heat transfer for low Reynold numbers. Moreover, for a heat exchanger with parallel channels, 3D effects in the solid walls and in the fluid significantly modify the heat transfer behaviour, and this cannot be predicted by correlations, which are obtained under the simplified boundary conditions of CWT or CWHF. Hence, the use of an accurate numerical simulation is often the only approach which can obtain good predictions of the fluid flow and heat transfer.

In conclusion it can be said that:

- conjugate heat transfer is a relevant phenomenon in microchannels and its influence has always to be checked;
- the criterion of Maranzana et al. [43], eq. (9), can be employed to define the condition for conjugate heat transfer effects being negligible. This needs to be verified by further research and comparisons.

2.6 Viscous heating

The energy equation for an incompressible fluid can be expressed as:

$$\rho_f c_p \frac{\partial T_f}{\partial t} + \rho_f c_p u_f \cdot \nabla T_f = \nabla \cdot \left(k_f \nabla T_f\right) + \phi \tag{10}$$

where ϕ, eq. (11), is the dissipation function, representing the irreversible conversion of mechanical energy to internal energy as a result of the deformation of a fluid element.

$$\phi = \frac{1}{2} \mu_f \nabla u_f \cdot \nabla u_f \tag{11}$$

In fluid flow with heat transfer inside a duct, the dissipation function is usually neglected. However, when the hydraulic diameter is very small, the internal heat generation due to the viscous forces can produce a temperature rise even if the flow is originally adiabatic. The temperature variation due to the viscous dissipation changes the values of the fluid thermophysical properties between the inlet and the outlet, and can remarkably influence the heat transfer. The Brinkmann number, which can be seen as the ratio between the viscous heating rate and the average heat transfer rate between the fluid and the channel walls, is usually employed to evaluate if the viscous heating effects can be influential. Depending on the boundary condition at the walls, it can be written as:

- $Br = \dfrac{\mu_f u_m^2}{k_f \left(T_w - T_f\right)}$ for CWT; (12)
- $Br = \dfrac{\mu_f u_m^2}{q_L}$ for CWHF; (13)

where u_m is the average flow velocity and q_L the heat transfer rate per unit length of the channel. The effects of the Brinkman number on Nusselt number depend on the characteristics of the boundary conditions.

Koo and Kleinstreuer [44] performed a numerical simulation of the flow in microtubes and microchannels, assuming steady laminar incompressible no-slip flow; they accounted for viscous dissipation and viscosity dependence on temperature. They pointed out that, as viscous dissipation increases rapidly, with respect to the other terms in the energy equation, its effects and that of viscosity variation with temperature have to be taken into account in experimental and computational analyses, especially in rectangular microchannels with low aspect ratio (zero aspect ratio indicating a channel between two parallel plates).

The papers of Jeong and Jeong [36], Chen [35], and Tunc and Bayazitoglu [38] have already been introduced in Section 2.3. They also analyzed viscous heating effects. Fig. 6, from Jeong and Jeong [36], shows the effects of viscous heating on the local Nusselt number, for Kn = 0 (i.e. no rarefaction effects) and $Pe = 10^6$ (i.e. negligible streamwise conduction). For constant wall temperature, fully developed Nu was independent of the Brinkmann number, but it was much higher than the value for Br = 0 (i.e. neglecting viscous heating effects). Fig. 6.A shows that Nu increases from 7.54 for Br = 0 to 17.5 for $Br \neq 0$. For constant wall heat flux, the Nusselt number varies with Br and can be lower for $Br > 0$ (i.e the channel is heated) and higher for $Br < 0$ (i.e. the channel is cooled). From Fig. 6.B it can be seen that Nu reduces from 8.24 for Br = 0 to around 7 for Br = 0.1.

Fig. 7.A shows the effects of rarefaction and viscous heating on the heat transfer reported by Chen [35]. When the viscous dissipation effect was accounted for, the local Nusselt number exhibited a jump at a certain axial position and then reached its final value. The increase for the Nusselt number, strong for non-rarefied flows ($\beta_v Kn = 0$), reduces significantly for increasing rarefaction. Fig. 7.B reports the effects of the Brinkmann number on heat transfer for a rarefied flow. Similarly to the findings of Jeong and Jeong [36], the Nusselt number increases also for rarefied flows, for $Br \neq 0$, to a value that does not depend on Br.

Tunc and Bayazitoglu [38], for the uniform temperature boundary condition and when the fluid is cooled by the walls, found that the fully developed Nusselt number increased to a value not dependent on Br, but higher than the corresponding one at Br = 0. When the heat is uniformly supplied to the fluid through the walls, increasing Br caused a decrease in Nu. Again, this behaviour agreed with that reported by Jeong and Jeong [36].

Viscous heating, as we have seen, was one of the scaling effects addressed by Morini [18] in his 2D steady laminar fully developed flow model with constant thermophysical properties. He showed that the temperature rise due to viscous heating is inversely proportional to the third power of the hydraulic diameter; hence, it could be very significant in microchannels. He proposed the following condition for having to account for viscous heating effects:

$$Br < \frac{\xi_{\lim} d_h^2}{2AfRe} \tag{14}$$

where $\xi_{\lim}$ is the maximum allowable ratio between the temperature rise due to viscosity and the temperature rise due to the supplied heat flux at the wall (for example, $\xi_{\lim} = 5\%$) and A the cross-sectional area. Moreover, as seen earlier, he analysed the effects of the entrance region and the conjugate heat transfer on the Nusselt number and proposed a map to evaluate the competing influence of different scaling factors on the Nusselt number (Fig. 5). He suggested that the dependence of the mean Nusselt number on the Reynolds number even in the laminar regime may be explained taking into account the conjugate heat transfer effects at low Reynolds numbers combined with viscous and entrance effects at high Reynolds numbers.

From the above cited results it is concluded that

- for flows with constant wall temperature, the Nusselt number increases, because of viscous heating effects, to a value that is not dependent on the Brinkmann number;
- for flows with constant wall heat flux, the Nusselt number decreases as the Brinkmann number increases;
- viscous heating can markedly influence heat transfer in microchannels, with different characteristics depending on the boundary conditions, and has always to be checked. Eq. (14), proposed by Morini [18], is suggested as a criterion to check whether viscous heating is negligible.

2.7 Surface roughness effects

At the microscale level, it is practically impossible to obtain what would be regarded in conventional engineering as a completely smooth wall surface. Nikuradse [45] and Moody [46] concluded, more than half a century ago, that if internal wall roughness is less than 5% of the channel diameter, its effects on the laminar flow characteristics can be ignored. But for microscale channels, the consistent conclusion of reported experimental and computational results is that surface roughness has a significant influence. For example, Mala and Li [47] observed that for rough tubes with diameters ranging from 50 to 254 μm and a relative roughness between 0.7 and 3.5%, the Poiseuille number $Po = f\ Re$, constant in fully developed laminar flows, increases with *Re*. Moreover, while most literature references on the role of surface roughness in the microscale regime agree in ascribing to it an increase in the Poiseuille number, much higher uncertainties arise when considering its effects on heat transfer.

Koo and Kleinstreuer [48] modelled the roughness in microchannels and microtubes as a porous medium layer (PML) to investigate numerically its effects on the friction factor and Nusselt number. Assuming steady laminar fully developed viscous flow with a porous medium layer, they found that the Nusselt number may be either higher or lower than the conventional value, depending on the surface roughness condition, but that this influence is less significant than on friction factor. They computed both lower and higher Nusselt numbers than the conventional values for both parallel plate channels and cylindrical tubes. They showed that the most important parameter affecting heat transfer, for a given surface roughness, is the thermal conductivity ratio between the porous layer and the fluid, with the Nusselt number increasing with this ratio. Furthermore, they showed a negligible influence of the Reynolds number and suggested that an experimentally observed dependence of *Nu* on *Re* has to originate from effects other than surface roughness.

In order to study the surface roughness effects on incompressible fully developed 2D flows in plane and circular channels, Croce and D'Agaro [49-50] explicitly modelled surface roughness through a set of randomly generated peaks along an ideal smooth surface, considering different peak shapes (squared and triangular) and distributions. An increase of the fluid velocity on the top of the peaks due to the local reduction in the cross-section, together with the boundary layer regeneration, locally increases the heat transfer. On the other hand, the recirculation zone in the following valleys reduces the local Nusselt number significantly. Thus, roughness may increase or reduce the global heat transfer rate depending on the relative importance of such effects, whilst it always increases friction losses. A small influence of roughness on heat transfer was found, often within the limits of accepted experimental uncertainty, except for very high roughness values which are unlikely in standard applications. A different behaviour between planes and circular channels was predicted. The former were found to have an increase in the Nusselt number with increasing roughness, while it reduces for the latter. Moreover, a higher reduction was calculated for triangular shaped roughness peaks than for square peaks. This high sensitivity to the surface details may help to explain the uncertainty in the literature regarding the effects of roughness on heat transfer. The authors suggested that great care is necessary in ascribing the discrepancies between experimental heat transfer data and predictions to surface roughness effects, without reliable information on the actual surface characteristics.

Ji et al. [51] numerically analysed the rarefaction, compressibility and surface roughness effects for a 2D pressure-driven gas flow between two long parallel plates, with uniform temperature, in the slip flow regime. The roughness was modelled by uniformly and symmetrically distributed rectangular blocks on the top and bottom surfaces of the channel. They found that increasing the roughness height leads to a pronounced decrease in the local heat flux for both rarefied and compressible flows. For rarefied flows the roughness elements penalize *Nu*, particularly at higher *Kn*. On the other hand, for a highly compressible flow, the average *Nu* does not change much or slightly increases, i.e. the existence of wall roughness enhances the heat transfer. Anyway, the influence of wall roughness on the average heat transfer is smaller than that on the Poiseuille number. The authors concluded that the wall roughness potentially causes a greater impact on the flow in the case of microchannels than for conventional channels. However, great care should be taken in ascribing to surface roughness discrepancies between experimental data for microchannels and macrochannels, as effects of roughness are always coupled with other competing effects, such as compressibility and rarefaction.

Shen et al. [52] carried out experiments for single-phase heat transfer in a heat sink with 26 rectangular microchannels (300 μm in width and 800 μm in depth), using deionized water as the working fluid. This was to study the effects of surface roughness, which was estimated to be 4-6% of the hydraulic diameter. The heat sink was made of copper, with 26 parallel microchannels constructed using a micromachining technique. Both the local and the average Nusselt number increased with increasing Reynolds number; notwithstanding, they were significantly lower than predictions of Shah and London [21] for all flow rates. This was attributed to a combination of cross-sectional aspect ratio and surface roughness effects. However, it will be shown later in Section 3 that these results should be ascribed *to conjugate heat transfer effects*, neglected by the authors, rather than to surface roughness.

The effects of aspect ratio, surface roughness and surface hydrophilic properties on apparent friction coefficient and Nusselt number for deionized water flowing in trapezoidal microchannels was studied by Wu and Cheng [53]. The Nusselt number was found to increase with increasing surface roughness. At very low Reynolds numbers ($0 < Re < 100$) the Nusselt number increases acutely and almost linearly with the Reynolds number, this increase being gentler for $Re > 100$. Correlations for the apparent friction factor and Nusselt number as functions of aspect ratio, surface roughness and hydrophilic properties, other than of Reynolds and Prandtl numbers, were provided for trapezoidal microchannels, Fig. 8, as follows:

$$Nu = C_1 Re^{0.946} Pr^{0.488} \left(1 - \frac{W_b}{W_t}\right)^{3.547} \left(\frac{W_t}{H}\right)^{3.577} \left(\frac{r_s}{d_h}\right)^{0.041} \left(\frac{d_h}{L}\right)^{1.369} \tag{15}$$

for $10 < Re < 100$, $4.05 < Pr < 5.79$, $0 \le W_b/W_t \le 0.934$, $0.038 \le H/W_t \le 0.648$, $3.26 \cdot 10^{-4} \le r_s/d_h \le 1.09 \cdot 10^{-2}$, $191.77 \le L/d_h \le 453.79$. $C_1 = 6.7$ for silicon surfaces and $C_1 = 6.6$ for thermal oxide surfaces.

$$Nu = C_2 Re^{0.148} Pr^{0.163} \left(1 - \frac{W_b}{W_t}\right)^{0.908} \left(\frac{W_t}{H}\right)^{1.001} \left(\frac{r_s}{d_h}\right)^{0.033} \left(\frac{d_h}{L}\right)^{0.798} \tag{16}$$

for $100 < Re < 1500$, $4.44 < Pr < 6.05$, $0 \le W_b/W_t \le 0.934$, $0.038 \le H/W_t \le 0.648$, $3.26 \cdot 10^{-4} \le r_s/d_h \le 1.09 \cdot 10^{-2}$, $191.77 \le L/d_h \le 453.79$. $C_2 = 47.8$ for silicon surfaces and $C_2 = 54.4$ for thermal oxide surfaces. Fig. 8 shows the geometrical characteristics and the nomenclature for eqs. (15)-(16).

Fig. 9 shows the Nusselt number, as a function of the Reynolds number, for several values of the relative roughness r_s/d_h, based on eq. (15) and (16) above. The surface roughness has a weak influence on the experimental Nusselt number, as in the numerical papers [48-50]; for example, for $Re=1500$, Nu reduces from 2.05 for $r_s/d_h = 0.001$ to 1.90 for $r_s/d_h = 0.01$. This could be considered as further confirmation that the significant reduction in Nu reported by Shen et al. [52] should not be ascribed to surface roughness.

Overall, it may be concluded that

- the surface roughness seems to have a weak influence on heat transfer in microchannels, often within experimental uncertainties, and depending on cross-sectional geometry, since the Nusselt number can both increase and decrease. Because of these weak and ambiguous effects, it is suggested not to perform any corrections to account for surface roughness on heat transfer.

2.8 Electric Double Layer (EDL) effects

According to Mala et al. [54], some of the deviations from macroscopic behaviour which have been reported for liquid flows could be explained with the *electric double layer* (EDL) effects. Most solid surfaces have electrostatic charges, i.e. an electrical surface potential. If the liquid contains very small amounts of ions, the surface charges will attract the counterions in the liquid to establish an electric field. The arrangement of the electrostatic charges on the solid surface and the liquid is called the *electric double layer* (EDL), as shown in Fig. 10. Because of the electric field, the ionic concentration near the solid surface is higher than that in the bulk liquid. In the compact layer, which is about 0.5 nm thick, the ions are strongly attracted to the wall surface and are immobile. In the diffuse double layer the ions are less affected by the electric field and are mobile. The thickness of the EDL ranges from a few nanometres to 1 μm, depending on the electric potential of the solid surface, the bulk ionic concentration and the temperature of the liquid.

When a liquid is forced through a microchannel, the ions in the mobile part of the EDL are carried towards one end, thus causing an electric current, called the streaming current, to flow in the direction of the liquid flow. The accumulation of ions downstream sets up an electric field with an electric potential called the streaming potential. This field generates a current, termed the conduction current, to flow back in the opposite direction. When the streaming and the conduction currents are equal, a steady state is reached. It is easy to understand that the conduction current tends to pull the liquid in the direction opposite to the flow. Thus, it acts as an additional drag force which increases the pressure drop and also affects heat transfer.

The Debye-Huckel parameter, κ, is used to characterize the EDL effects:

$$\kappa = \sqrt{2 n_0 z^2 e^2 / \varepsilon \varepsilon_0 k_b T_f} \tag{17}$$

where n_0 is the ionic number concentration, z is the valence of the positive or negative ions, e = 1.6021x10^{-19} C is the electron charge, ε is the relative permittivity of the medium, ε_0 is the permittivity in vacuum, k_b is the Boltzmann constant and T_f is the fluid temperature. $1/\kappa$ is usually referred to as the characteristic thickness of the EDL. When the EDL thickness is a non-negligible fraction of the hydraulic diameter its effects should be taken into account. More specifically, a source term has to be added in the momentum equation for the direction of flow, representing the electric body force due to the streaming potential:

$$F_{EDL} = \rho_{el} E_s \tag{18}$$

where ρ_{el} is the electric density and E_s the electric field due to the streaming potential.

Mala et al. [54] simulated a 1D flow between two parallel plates and showed that neglecting the EDL effect led to an overestimation of the local and average *Nu*. The authors strongly recommended that EDL effects should be accounted for in the design of microdevices.

Ng and Tan [55] and Tan and Ng [56] developed a numerical model which accounts for the EDL effect on 3D developing flow in rectangular microchannels. They characterized the EDL effects by means of the parameter $K = \kappa \cdot d_h$, which can be seen as the ratio between the hydraulic diameter of the channel (d_h) and the EDL thickness ($1/\kappa$). They found that EDL effects can modify the cross-section velocity profile, increase the developing length and the wall temperature, for a CWHF boundary condition. Hence the friction coefficient increases and Nusselt number decreases. This suggests a similar effect to that of the viscosity. For example, for $K = 100$ and $K = 20$, they found fully developed Nusselt numbers of 4.1225 and 3.2823 respectively, while when neglecting EDL effects it is equal to 4.4523. The overprediction in Nu goes from 8% for $K = 100$ up to 35% for $K = 20$, i.e. for thicker EDL layers. It is pointed out that a comprehensive thermal model for a microchannel should consider EDL phenomena.

It is concluded that:

- EDL effects can sensibly influence heat transfer in microchannels and should be taken into account when the EDL thickness is a non-negligible fraction of the hydraulic diameter;
- based on the work of Ng and Tan [55] and Tan and Ng [56], the following criterion is proposed to state whether EDL effects should be considered:

$$K < K_{\text{lim}} \tag{19}$$

where K_{lim} depends on the maximum allowable EDL thickness relative to the hydraulic diameter. For example, when K_{lim} is equal to 100 or 20, the EDL thickness is, respectively, 1% or 5% of the hydraulic diameter.

Finally, it must be remembered that EDL effects are relevant only for liquid flows containing ions and when the wall surface bears an electrostatic potential.

2.9 Measurement uncertainties

All of the cited reviews about microchannels [9, 12, 14-17] agreed that one possible explanation of the discrepancies between experimental and theoretical results, other than the above listed scaling effects, is the experimental uncertainty which may significantly reduce the reliability of the measurements. Morini [12], in particular, concluded that, because of experimental uncertainties, much of the earlier published results may be unreliable and not useful for comparisons. He underlined that the most recent experiments, where scaling effects and measurement uncertainties can be more accurately checked, are in closer agreement with classical theory and predictions. Celata [9] listed several sources of experimental uncertainty:

- lack of accuracy in diameter measurement, combined with its variation along the channel due to manufacturing difficulties. For example, in laminar flow, the heat transfer coefficient is inversely proportional to the diameter and an error in its measure will directly influence the comparison between measured and calculated heat transfer coefficients;
- the increasing difficulty in determining fluid and channel wall temperatures as the length scale decreases. Moreover, the thermocouples that are often used as temperature sensors may have dimensions of the same order of magnitude as the channels themselves, probably affecting the temperatures to be measured;
- the fact that tests are usually done with several channels connected in parallel. Hence the results could be influenced by maldistribution issues and the measurement of a representative channel wall temperature is especially difficult;
- the classical correlations are valid only under idealised conditions of either constant surface temperature or constant heat flux. These conditions may be difficult to achieve in a microchannel, especially when using a multi-channel configuration.

Several experimental works published in the last few years will now be reviewed and the related uncertainties discussed.

Bucci et al. [22], using a single, stainless steel, microtube, obtained friction factor and Nusselt numbers for degassed and demineralised water, with the Reynolds number ranging from 200 to 6000. Three tube diameters were tested (172, 290 and 520 μm). For the heat transfer experiments, the microtubes were heated by direct condensation of water vapour on the outer surface of the tube, so their wall temperature was maintained constant at the value of the saturation temperature of the water. The uncertainty in the Nusselt number was evaluated as equal to ±22.25%. In the laminar flow regime, the Nusselt number deviated from the Hausen correlation [23] (as given in section 3) for thermally developing flow. The largest microtube showed an increase of Nusselt number up to 17% higher than that predicted, while the smallest one deviated by up to 55% higher than the predicted value. In the turbulent flow regime, 520 μm and 290 μm microtubes showed quite good agreement with the Gnielinski correlation [57], while for the 172 μm one there were very few experimental points in the turbulent regime, which seem to be significantly higher than the Gnielinski [57] correlation and in good agreement with that of Adams et al. [10].

Another investigation into flow and heat transfer through an individual circular microchannel ($d_h = 0.8, 1.2$ and 1.7 mm, *Re* = 1000-17000) was due to Owhaib and Palm [58]. Using R143a as the working fluid, they measured the heat transfer coefficient and the Nusselt number and tested the predictive capability of several correlations for macro- and micro-channels. The uncertainty in the temperature differences between the fluid and the wall was estimated to be ± 0.2 °C, but no information was given about the uncertainty in the Nusselt number. The experimental results were in good agreement with the macro-scale correlations and disagreed with all of the micro-scale correlations; the large tube diameters (1.7, 1.2 and 0.8 mm) of their experiments could probably account for the result of this comparison.

Gao et al. [20] investigated heat transfer and fluid flow in deep rectangular microchannels with hydraulic diameters ranging from 0.2 to 2 mm and Reynolds numbers from 100 to 8000. Fig. 11 shows a sketch of the test section they used to perform the experiments. The active channel walls are two plane brass blocks, separated by a foil; the thickness of the foil fixes the channel height. Heating of the fluid was provided by four electric cartridges inserted inside the two blocks. Each heating block was mounted in a housing machined in a larger block of total thickness 30 mm and surrounded by 5 mm of epoxy resin as insulating material. The brass blocks were equipped with five thermocouples of type *T* (diameter = 0.5 *mm*) placed every 15 *mm* apart, whose sensitive part was located 1 *mm* away from the metal-fluid interface. The inlet/outlet temperatures were measured by thermocouples of type *K*. The maximum uncertainty in the Nusselt number was estimated to be around 8%. The Nusselt number satisfactorily agreed with the Shah and London data [21] for hydraulic diameters higher than 1.0 mm, while it showed a reduction for the smaller thickness, up to 30% for d_h = 0.2 mm.

The experimental apparatus of Gao et al. [20] was considered in the papers of Gamrat et al. [42] and Bavière et al. [59]. Gamrat et al. [42] performed detailed numerical analysis of the experimental system, modelling its 3D geometry and accounting for entrance effects and 3D conjugate heat transfer in the fluid and the solid walls. Nevertheless, they couldn't predict the reduction in *Nu* for d_h < 1 *mm*. Bavière et al. [59] recalculated the experimental uncertainty and found that it may have been up to 20%

for Re < 3000 and up to 50% for Re > 3000. Moreover, they performed a complementary experiment that allowed them to estimate the bias effects on the wall temperature measurement due to the thermal contact resistance between the thermocouple junction and the brass of the solid blocks. When the measured wall temperatures were corrected to account for the thermal contact resistance effects, the Nusselt numbers were in good agreement with the Shah and London [21] data also for $d_h < 1$ *mm*, and the authors could show that the deviations between the experimental results of Gao et al. [20] and the theoretical predictions were due to wrong estimations of the channel temperature.

Celata et al. [24] investigated single-phase heat transfer for water flows in single microtubes with diameters ranging from 528 down to 50 μm and Re from 50 to 2775. The experimental apparatus was designed in such a way as to reduce the experimental uncertainties as much as possible. The microchannel was mounted inside a vacuum capsule to avoid convective heat losses to the surroundings; the heat losses due to radiation, to axial conduction in the walls and to viscous heating were estimated to be negligible as well. The average Nusselt number increased with the average Reynolds number, because of entrance effects. For the 528 μm diameter, the experimental Nusselt number agreed with predictions of the Hausen correlation [23] (given in section 3) for thermally developing flows, while for lower diameters it was increasingly smaller than predictions. The authors stated that, at reducing diameters, the heat losses through elements outside of the system boundaries (thermocouples, fittings, connected tubing) become increasingly relevant and may lead to significant measurement errors. In fact, for the 50 μm diameter tube, the sensitivity to measurement errors was so large that it was impossible to obtain a realistic estimate of the heat transfer coefficient.

Liquid crystal thermography was proposed by Muwanga and Hassan [25] for local heat transfer measurements in microchannels (d_h = 1 mm, Re = 600-4500). Using an airbrush to coat uniformly the outer surface of the microtube with unencapsulated thermochromic liquid crystals and after an accurate calibration, they found that the Nusselt number for deionized water flow in a 1 mm diameter microtube with constant heat transfer wall flux was in good agreement with the analytical solution of Shah and London [21] for thermally developing flows in the laminar regime and with the Gnielinski correlation [57] in the turbulent regime. On the other hand, the uncertainty in the Nusselt number evaluation was estimated to be up to 23.7%, due to the considerable noise in the measurements.

Lelea et al. [26] studied heat transfer and fluid flow for distilled water in the laminar regime. They used single circular microchannels with 125.4, 300 and 500 μm diameter and Re in the range 100-800. The tube was mounted inside a vacuum chamber to reduce convective heat losses to the surroundings and the experimental uncertainty in the channel diameter and the heat transfer coefficient h were estimated, in the worst case, as 5.6% and 8.9% respectively. They found good agreement between measured Nusselt numbers, their own numerical predictions and analytical results (Nu = 4.36, for fully developed laminar flows). The data also agreed with the Shah and London correlation [21] for thermally developing laminar flows.

Lee et al. [19] investigated heat transfer in rectangular microchannels of different hydraulic diameters (318-903 μm), for Re = 300-3500, using deionized water. The heat sink was made of copper with ten machined parallel microchannels. The experimental uncertainty in the Nusselt number was estimated to be in the range 6-17 %. The Nusselt numbers they obtained were found to be in disagreement with *all* of the ten tested correlations for heat transfer available in the open literature, while the authors found good agreement between their experimental results and their own numerical predictions, where they were able to better match the boundary conditions and entrance effects with those of the real flow.

Shen et al. [52] carried out experiments for heat transfer in a heat sink with 26 rectangular microchannels (300 μm width and 800 μm depth), for Reynolds numbers between 162 and 1257, using deionized water as the working fluid. The heat sink was made with copper and the microchannels were constructed using a micromachining technique. The authors assumed an identical behaviour between the 26 microchannels and neglected solid heat conduction in the flow direction. The fluid properties were calculated at the mean temperature between inlet and outlet. The maximum experimental uncertainty in the Nusselt number was declared equal to 5.93%. Both the local and the average Nusselt numbers increased with increasing Reynolds number due to thermally developing laminar flows, but were significantly lower than the conventional theory predictions for all flow rates.

The effects of aspect ratio, surface roughness and surface hydrophilic properties on Nusselt number for deionized water flowing in trapezoidal microchannels ($d_h = 65-160$ μm, *Re* = 10-1500) was studied by Wu and Cheng [53]. The surface hydrophilic properties were changed using silicon surfaces or by coating them with a layer of silicon oxide (SiO_2). The experimental uncertainty in *Nu* was estimated to be up to 7.82%. The Nusselt number was deeply influenced by the geometrical characteristics of the cross section and increased with increasing surface roughness and hydrophilic properties. Finally, correlations for the friction factor and the Nusselt number as functions of aspect ratio, surface roughness and hydrophilic properties, other than of Reynolds and Prandtl numbers, were provided. No comparisons with existing correlations were made.

The review is briefly summarized in Table 2, where experiments with single microchannels are clearly separated from those with parallel microchannels . Nu_{pr} is the Nusselt number predicted using correlations for large channels.

From the above review, several overall observations can be made:

- scaling effects are almost always carefully evaluated;
- experiments with <u>single circular microchannels</u> are usually more accurate and in good agreement with standard correlations;
- new sources of experimental uncertainties have been found to be significant, like thermal contact resistance for thermocouples [59] and heat losses through connections and wires [24];
- for single channels, the agreement between experimental results and predictions tends to deteriorate for decreasing hydraulic diameters ($d_h \leq 300-500\ \mu m$).
- the largest discrepancies arise with parallel channels, probably because of maldistribution effects and badly evaluated entry effects, and experimental systems with insufficient thermal insulation.

3. SCALING EFFECTS IN THE DESIGN OF MICROCHANNELS

The review carried out above has highlighted, consistently with Hetsroni et al. [14], that *there are no new phenomena in heat transfer in microchannels, but the scaling effects and the measurement uncertainties can have a strong influence*. Therefore, great care has to be used to estimate their influence when analysing the experimental results; otherwise, an incorrect representation of the physical reality may lead to wrong conclusions in the interpretation of experimental results. As an example, we may consider the work of Shen et al. [52]. The tested heat exchanger was made of 26 identical microchannels with rectangular cross-section. Fig. 12 depicts the cross section of the channels and includes the relevant geometric characteristics. The microchannels were made in a copper block using a micromachining technique. The relative roughness was estimated to be 4%. The top surfaces were obtained by means of a glass cover plate. The heat to the channels, *q*, was supplied from the bottom surface of the copper block. The average Nusselt number was significantly lower than the predictions obtained with the Shah and London correlation [21]. The authors attributed this behaviour to surface roughness effects. The data reduction performed by the authors was based on several simplifying assumptions:

1. each parallel microchannel has exactly the same size and wall roughness;
2. flow rates in each microchannel are the same;
3. heat conduction in the solid copper block along the flow direction is neglected;
4. the heat flux for each microchannel is the same.

These assumptions are quite profound for the geometric configuration of the test section and lead to a complete neglect of the effects of maldistribution that may be relevant in a heat exchanger with 26 parallel microchannels. Moreover, conjugate heat transfer effects were totally neglected, but the Maranzana number *M*, according to eq. (8) and because of the geometric dimensions, is in the range 2-20. According to eq. (9), the conjugate heat transfer effects have a significant influence and yield a reduction in the Nusselt number. On the other hand, section 2.5 has underlined that surface roughness effects on heat transfer are quite weak. Hence, after a more accurate analysis of the experimental setup, the reduction in the Nusselt number may be attributed to conjugate heat transfer effects, instead of surface roughness effects.

The design of heat exchangers makes an extensive use of correlations, available in the open literature for different kinds of heat exchangers and geometric configurations. Some of these are included here, in Table 3, for ease of reference. For heat transfer inside ducts, several robust correlations have been developed, for different flow regimes and boundary conditions and cross-section geometries. In the laminar regime, it can be shown theoretically that, for 1D flows, the Nusselt number for fully developed flow is a constant whose value depends only on the boundary condition and the cross-section geometry. Hence, when comparing with experimental results, the first step is the choice of the most suitable correlation for the cross section and the boundary conditions used.

Moreover, the influence of the entrance effects should always be checked and, eventually, taken into account. Equations (20)-(23) in Table 3 give the correlations for the average Nusselt number in thermally developing flows in circular channels proposed by Hausen [23] and Shah and London [21].

Correlations and data for different cross-sections may be found again in the work of Shah and London [21]. For turbulent flows, the entry lengths are considerably shorter than their laminar flow counterparts [60] and correlations for fully developed flows are usually employed. Moreover, these correlations can be used for different cross section geometries and boundary conditions. Equations (24-25), (26) and (27) give the correlations of Gnielinski [57], Dittus and Boelter [61] and Pethukov et al. [62], respectively.

The suitability of these correlations, developed for large-sized channels, has been deeply questioned for microchannels, since they seemed unable to predict the Nusselt number. As a consequence, several correlations, specific for microchannels, have been proposed and some of them are reported in Table 3, equations from (28) to (31). On the other hand, this review has shown that heat transfer in microchannels can be predicted by classical theories, once scaling effects and measurement uncertainties are taken into account. Correlations for laminar flows in circular channels are compared in Fig. 13.A. The Shah and London [21] and the Hausen [23] correlations are in close agreement for the CWT boundary condition, while their predictions differ by up to 30 % for CWHF. However, the correlation of Choi et al. [63], proposed specifically for microchannels, shows a trend of variation of *Nu* with *Re* which is completely different from those of other authors. Analogous conclusions may be drawn for other cross-sectional geometries. Based on the results of the present review, and since the correlations specifically proposed for microchannels were usually derived from a best-fit of the experimental results but without explicitly taking into account the scaling effects, they may need further verification or improvement before they can be used generally for the prediction of the laminar heat transfer in microchannels.

Less information is available about the suitability of classical correlations to predict the heat transfer in microchannels in the turbulent regime. Only a few of the examined papers presented results for the turbulent regime and they agree sometimes with the classical correlations of Gnielinski [57], Dittus and Boelter [61] and Pethukov [62] and sometimes with the correlation of Adams et al. [10], proposed specifically for microchannels. Fig. 13.B shows the *Nu-Re* curves given by different correlations. The classical correlations of Gnielinski [57], Dittus and Boelter [61] and Pethukov et al. [62] are in reasonable agreement with each other, within 20 % for $Re > 3000$. The correlations of Choi et al. [63] and of Yu et al. [64], proposed for microchannels, show completely different trends of variation for *Nu* with *Re* both with the standard correlations and with themselves. As in the laminar regime, they need further verification and improvement before general use. In contrast to them, the correlation of Adams et al. [10] is not a “new” correlation for microchannels but only introduces a correction to the Nusselt number predicted by the Gnielinski’s correlation, based on the value of the hydraulic diameter, when the latter is lower than 1.2 mm. The experimental results of Bucci et al. [22] in the turbulent regime, for example, were in good agreement with the Gnielinski’s correlations for d_h = 520 and 290 μm and with the Adam’s correlation for d_h = 172 μm. Hence, although more of the examined papers are in good agreement, in the turbulent regime, with the classical correlations, further research is needed to clarify whether the Adam’s correlation is reliable or not.

Summarizing, since there are seem to be no new phenomena in microchannels, the classical correlations or data of Hausen [23] or Shah and London [21] to predict the heat transfer in thermally developing laminar flows may safely be used, *but only for 1D flows and when all the scaling effects can* *be neglected*. For turbulent flows, the suitability of the classical correlations of Gnielinski [57], Dittus and Boelter [61] and Pethukov et al. [62] is still an open matter, but based on the results of this review they seem to be quite reliable at least for d_h > 300-500 μm.

Table 4 reports the criteria and/or suggestion to state whether a particular scaling effect is negligible. If one of the scaling effects cannot be neglected, predictions have to be corrected. To the best of the authors' knowledge, these corrections can be performed only for a few specific cases (for example, for viscous heating in rectangular microchannels [18]); in the general case, suitable numerical simulations have to be performed. Great care has to be taken in gas flows, because in highly rarefied flows ($Kn > 0.1$) the Navier-Stokes equations are no longer valid and molecular models have to be employed (see Section 4).

When undertaking the design of a microchannel heat exchanger, where many *parallel microchannels* are used, correlations may only give a gross estimation of the Nusselt number. Even when the above-introduced scaling effects are accurately considered and can be neglected, there is flow maldistribution between the channels [65] and 3D conjugate heat transfer patterns in the solid and the fluid [41], whose effects may be significant but cannot be accounted for by standard correlations, developed for 1D flows with simplified boundary conditions. For these reasons, the design of heat exchangers with microchannels cannot be reliably made without performing accurate numerical simulations, also to address the 3D effects in the inlet and outlet manifolds and in the solid and fluid heat flow patterns. Otherwise, the heat transfer coefficient should be measured by means of a dedicated, well designed experimental apparatus. Lee et al. [19], for example, carried out experiments on a heat exchanger with ten parallel microchannels, and compared the results with several correlations and numerical simulations. They obtained good agreement only when considering 3D conjugate heat transfer effects or when using the "thin wall" boundary condition (axially uniform heat flux with circumferentially uniform temperature). This matches the boundary condition of the flow much better than the standard CWT or CWHF conditions.

In conclusion, it is strongly recommended to use numerical simulations in the design of heat exchangers with parallel microchannels, since they are the sole option to accurately describe scaling, maldistribution and 3D effects. Correlations may only be used in the initial stage of the design process for approximate and preliminary estimations. Otherwise, if a precise knowledge of the heat transfer coefficient is needed, an experimental campaign has to be carried out using an accurate and well-designed test rig.

4. MODELLING OF SUB-CONTINUUM EFFECTS

An underlying assumption of this review (as noted in the beginning of Section 2) is that the fluid is treated as a continuum. However, as also noted in 2.3, the assumption is not always valid, with expressions such as 'rarefaction effects', 'slip flow' and 'temperature jump at the wall' used as indicators. For example, for air at standard temperature (288 K) and pressure (1 atm), the mean free path λ = 0.065

μm; hence, a microchannel with a hydraulic diameter of 1 μm would have Kn = 0.065 and be in the slip flow regime. This is summarised in Fig 14.

We now explain, rather than review, the status of modelling developments for the sub-continuum region. These developments seek to address the fundamental molecular structure of a fluid. However, in a fluid continuum, the number of molecules at a given scale is sufficiently large, and individual molecular effects are 'smoothed out' and indistinguishable. The Navier-Stokes (N-S) equations address this continuum condition very well, with a universality of no known upper limit. It is not surprising, therefore, that microchannel heat transfer is modelled by these equations. This is despite Gad-el-Hak's caution that 'the small length-scale of microdevices may invalidate the continuum approximation altogether' [29]. In this section it will be consistently noted that sub-continuum conditions for dilute/rarefied gases and for liquids represent somewhat divergent fields of study. One aspect of this is that for the former, the condition of thermodynamic equilibrium, also required for validity of the N-S equations, breaks down, for dilute gases, well before the continuum condition does [29].

There are two main reasons for the continuum approach being more likely to be inadequate for the future. Firstly, within the microchannel scale range dimensions are steadily reducing with time, from the upper limit which verges on conventional behaviour down to scales approaching the nano. Molecular behaviour is becoming correspondingly more important and Gad-el-Hak's above caution becomes increasingly justified. Secondly, the molecular description is more fundamental and, as made clear below, molecular-based models *accommodate and can address continuum situations*. In fact, to anticipate, the most commonly used model, the Lattice-Boltzmann (LB), is even being promulgated as being *better than the N-S* at resolving turbulent flow for engineering problems. The following description, although concise, has to be comprehensive. This is partly because key terms such as 'transitional' and 'macroscopic/microscopic' have mathematical and not conventional fluid dynamics meanings.

The Knudsen number has already been defined in Section 2.3 and its ranges for the various regimes shown in Fig. 14. The slip boundary condition regime means that the continuum can still be used, but needs adaptation adjacent to the wall. As noted above, the term 'transition' is used in a mathematical sense to describe a regime where the continuum concept finally breaks down and molecular effects must be accommodated. The basic modelling implications for these ranges are given below, and it is possible to envisage all but the highest regime being relevant to microchannel thermofluids problems. This point is exactly made by Gad-el-Hak [29] in the context of a postulated *single long microchannel.*

The various models are classified in mathematical terms as being macroscopic (continuum based), microscopic (based on individual molecules) or mesoscopic (with characteristics of both). It is somewhat unfortunate that these terms conflict with the engineering classification of microchannels.

We now distinguish between the three types of models in the context of fluid flow and especially in the precise meaning of the *fluid particle addressed.* The *macroscopic* model relates to flow variables such as density, velocity and pressure. On the continuum assumption, the particle is a fluid element, which no matter how small, still retains the bulk fluid properties [29, 66]. The *microscopic* model relates to individual molecules, atoms or ions, these simply defining the microscopic particle. The *mesoscopic* model relates to groups of individual molecules. It fits between the microscopic and macroscopic models, being based on a simplification of the MD approach combined with some of the continuum ideas used in deriving the NS equations. The rationale for the mesoscopic approach includes the consideration that macroscopic properties do not directly depend on microscopic behaviour. The mesoscopic fluid 'particle' is a large group, or cluster, of molecules which is considerably smaller than the smallest length scale of the simulation in question. The definition is rather subtle, and use of such expressions as 'pseudo-particle' ([67], 2) 'fictive particles' ([67], 2, 1) and 'fictitious computational quasi-particles' ([68], 635, 1) may be noted!

What is already being widely applied in engineering, and may ultimately emerge as a very useful approach for microchannel thermofluids, is the Lattice Boltzmann (LB) model. This is mesoscopic in concept, as is another, the DSMC (Direct Simulation Monte Carlo) method. Haas[67] sub-divides the mesoscopic 'pseudo particle' approach into lattice based (e.g. LB) and off-lattice (e.g. DSMC) models.

Thermofluids researchers are accustomed to working with the NS equations together with the corresponding pde's (partial differential equations) for energy (frequently) and species (more occasionally). The basis for them is barely addressed in publications. In fact there is a range of theoretical methods available and the relationships between them are shown in Fig. 15. This is adapted from Gad-el-Hak [29], who also gives a thorough explanation of the models, together with the relevant pde's. Again, for advanced understanding, this reference is particularly valuable as it is written within an engineering (MEMS) context.

Three key points should be made. Firstly, for an absolute molecular, or microscopic, description MD (Molecular Dynamics) is available, especially for 'dense gases and liquids' [29]. However, the computational demands of resolving individual molecules are so heavy that only very small volumes can be addressed. Secondly, the mesoscopic methods both have a statistical basis ('the fraction of molecules in a given location and state is the sole dependent variable' [29]) rather than the deterministic MD. They are based on the Liouville equation [29]. The Boltzmann equation, 'the fundamental relation of the kinetic theory of gases' [29] stems from this. The DSMC is 'a random number strategy' which 'uncouples the molecular motions and their collisions' and is 'valid for all Kn' but 'expensive for Kn <1'[29]. Gad-el-Hak [29], despite giving a good description of the basis for the LB approach, focuses on DSMC to the virtual exclusion of LB. This is consistent with his comment, as at 1999, that 'the microfluid mechanics of liquids is much less developed than that for gases' [29]. The study of Xue et al. [69] is similar. For the microchannel researcher this DSMC focus should be balanced by knowledge of the material in the 2003 and 2005 publications of Haas [67] and Buick et al. [70] respectively of the LB literature. Thirdly, however, Gad-el-Hak very helpfully points out that the entire macroscopic model range results from the Boltzmann equation via Chapman-Enskog theory [71, 72]. Within this: 'the zeroth-order equation yields the Euler equations, the first-order equation results in the linear transport terms of the NS equations, the second-order equations give the non-linear transport terms of the Burnett equations, and so on' [29]. The same theoretical message is inherent in the briefer report of Chen et al. [68]. They, however, focusing on turbulent flow, apply to the Boltzmann equations the 'collision operator introduced by Bhatnagar, Gross and Krook (BGK)' [73]. From this the NS equations are obtained as: 'the low-order truncation of the expansion of the Boltzmann/BGK equation in powers of Kn', that is, a 'second-order truncation'. For higher Kn the expansion leads to an infinite hierarchy of pde's with various higher-order terms known as the Burnett equations' [68]. Unlike DSMC, the LB approach does not give so much a 'quantitatively correct description of fluids to all orders in Kn' but rather is 'better than any finite-order truncation of the series' [68]. This is radical, being the basis for claiming the LB method is *preferable to the NS equations for turbulent flows.* In the context of applying CFD to problems in materials science, a more general claim is made by Haas [67] that: 'the LB techniques seem to be predestined to tackle some of these challenges in a more efficient way than the NS approach'.

The above discussion reveals different emphases in the DSMC and LB publications.

An attempt is now made to unify the models on the basis of their engineering applications. Taking Gad-el-Hak's review as dominant, Table 5 lists recommended models as a function of *Kn*, firstly for gas flows. The statement by Haas confirms that 'the particular strength of the DSMC lies in the field of dilute gases' [67] and his abbreviated range presentation [67] is also shown in Table 5 for liquids.

Table 5 reflects most of our preceding discussion and represents an overall set of recommendations for the use of the various models. Researchers in thermofluids, and especially those using CFD, tend to take the NS equations as they stand. With both the increasing use of, and more importantly the necessity for, molecular based models, an appreciation of their relationship with continuum models is needed. This section attempts to give such an appreciation, largely inspired by the almost exhaustive review of Gad-el-Hak [29]. For the LB model in particular, a more important future has been advanced both within and beyond the bounds of microchannels. Haas [67] and Buick et al. [70] list many applications in diverse fields of fluids. A number of these are in medical flows: referenced here are the review of Buick et al. [70] and a very recent example, Galbusera et al. [74]. It is worth noting that Galbusera et al. feel the approach is sufficiently novel to have to justify it by, especially, reference to Succi's LB work. Succi is also the corresponding author of [68], which promulgates LB as better for turbulent flows than conventional NS-based turbulence modelling. The applications are core engineering problems, flows over a high-performance car and NACA aerofoils.

5. CONCLUSIONS

5.1 Detailed conclusions

Numerical and experimental results for heat transfer in microchannels have been reviewed. Despite the existing discrepancies between published results, it has been shown that standard theories and correlations are suitable to describe heat transfer in microchannels, once cross-section geometry, scaling effects and measurement uncertainties are carefully considered.

In particular, the following scaling effects have been found to be significant and their influence on heat transfer performances can be summarized as follows:

- <u>entrance effects</u>. The thermal entry length is usually a significant fraction of the total length of the microchannel and effects on heat transfer have to be considered. Hence, correlations for developing flows have to be used for the calculation of the Nusselt number;

- temperature dependent properties. When the variation in fluid temperature between the inlet and the outlet of the microchannel is sufficient to change the fluid properties, especially the viscosity, these have to be accounted for;
- rarefaction effects (only for gas flows). For rarefied flows, the Nusselt number varies because of slip flow and temperature jump at the walls. Slip flow tends to increase *Nu*, while temperature jump tends to decrease it. Hence, if wall temperature jump could be neglected, rarefaction effects would lead to increased heat transfer, but in typical engineering applications, when slip flow is always accompanied by a temperature jump at the wall, rarefaction causes a reduction in the Nusselt number;
- compressibility effects (only for gas flows). For gas flows, compressibility effects have to be considered, even for $Ma < 0.3$, because strong pressure losses may lead to density variations with significant influence on the velocity and temperature profiles, and hence on heat transfer;
- conjugate heat transfer. The thickness of the solid walls of the microchannels is often of the same order of magnitude as the hydraulic diameter. This means that it is not possible to neglect solid axial heat conduction which, especially at low Reynolds numbers, reduces the Nusselt number. Moreover, when using parallel channels as in commercial micro-heat sinks, there is a strong coupling between the heat transfer by convection in the fluid and by conduction in the solid substrate, with significant 3D effects that must be considered. In these cases, good predictions may be achieved only by appropriate numerical simulations. The criterion of Maranzana et al. [43], eq. (9), is used to evaluate if conjugate heat transfer effects have to be taken into account;
- viscous heating. Viscous dissipation in the fluid can markedly influence heat transfer in microchannels. For a heated channel, the Nusselt number increases in flows with constant wall temperature and decreases in flows with constant wall heat flux. The criterion of Morini [18], eq. (14), is employed to state whether viscous heating effects have to be considered;
- surface roughness. Depending on the cross-section geometry and on the roughness shape the Nusselt number can both increase and decrease. However, these variations are always within the limits of experimental uncertainties. Therefore, it is reasonable to believe that surface roughness has no relevant effect on heat transfer, that unexpected experimental results should not be ascribed to it and that no corrections have to be performed to standard correlation predictions;
- EDL effects. In aqueous solutions, the electric double layer thickness can be a relevant fraction of the hydraulic diameter of the microchannel, so having an influence on heat transfer. Based on the results of Tan and Ng [56], eq. (19) is proposed as a criterion to state if EDL effects have to be accounted for.

Measurement uncertainties represent a key aspect for microchannel studies. For experiments with single channels and when all the scaling effects can be neglected, measurements yield Nusselt numbers in quite good agreement with the predictions using available correlations for macro-channels. On the other hand, when a heat exchanger with several parallel microchannels is used for experiments, this agreement strongly deteriorates because of maldistribution of flow and 3D conjugate heat transfer effects. These make standard correlations for the Nusselt number unreliable for exchanger design purposes.

Mathematically mesoscopic and microscopic models for sub-continuum effects in fluid flows have been reviewed and explained. These models still represent quite a large "work in progress" research area. Their more relevant characteristic is their promise to be more comprehensive, being based on the mathematical description of the fundamental molecular mechanisms. The continuum approach itself may be derived from these models and be considered as a special case. On the other hand, microscopic and mesoscopic models still require an enormous amount of computational resources and run times, which make them still unsuitable for typical, geometrically complex, industrial fluid domains. However, mesoscopic and microscopic models will have growing importance and diffusion in the near future, since microchannel sizes are steadily reducing and tend towards the nanoscale, where N-S equations approaches are no longer suitable and a particle approach becomes unavoidable.

5.2 Recommendations

For purposes of performance and design the following recommendations are made:

- classical theories of fluid flow and heat transfer are reliable, but the scaling effects must be accounted for;
- if the scaling effects can be considered negligible, and only when using a single channel, correlations such as Hausen [23] and Shah & London [21] may be used to predict the Nusselt number in thermally developing laminar flows. Certain correlations specific for microchannels need further verification/improvement;
- in the turbulent regime, further research is needed to state which one is the most suitable correlation. Both the classical correlations of Gnielinski [57], Dittus and Boelter [61], Pethukov et al. [62] and the microchannel correlation of Adams et al. [10] have been found suitable in certain situations. Classical correlations seem to be quite reliable for $d_h \geq 300 - 500$ μm;
- otherwise, if a good estimate of the Nusselt number is needed when the scaling effects are not negligible and/or with complex geometrical configurations (for example, heat exchangers with several parallel microchannels where maldistribuition and 3D conjugate heat transfer effects are often relevant), it is necessary to carry out either detailed 3D numerical simulations, where all the relevant phenomena can be modelled, or dedicated and accurate experimental campaigns.

Acknowledgment

The authors are most grateful to Dr. D. Lockerby at the University of Warwick for his help and advice during the preparation of the paper.

References

1. R.J. McGlen, R. Jachuck, S. Lin, Integrated thermal management techniques for high power electronic devices, Applied Thermal Engineering 24 (2004), 1143-1156.
2. P.E. Ross, Beat the heat, Spectrum, IEEE, Vol.41, Iss.5, May 2004, 38-43.
3. International Technology Roadmap for Semiconductors, Assembly and Packaging, 2005 Ed.
4. D. M. Tuckerman, R.F.W. Pease, High performance heat sinking for VLSI, IEEE Electron Device Lett., Vol. 2, No. 5, 126-129, 1981.
5. K. Schubert, J. Brandner, M. Fichtner, G. Linder, U. Schygulla, A. Wenka, Microstructure devices for applications in thermal and chemical process engineering, Microscale Thermophysical Engineering 5 (1) (2001), 17-39.
6. J.J. Brandner, E. Anurjew, L. Bohn, E. Hansjosten, T. Henning, U. Schygulla, A. Wenka, K. Schubert, Concepts and realization of microstructure heat exchangers for enhanced heat transfer, Experimental Thermal and Fluid Science 30 (2006), 801-809.
7. K. Nikitin, Y. Kato, L. Ngo, Printed circuit heat exchanger thermal–hydraulic performance in supercritical CO2 experimental loop, Int. J. of Refrigeration 29 (2006), 807-814.
8. P.M. Martin, W.D. Bennett, J.W. Johnston, Microchannel heat exchangers for advanced climate control, SPIE Vol. 2639 (1995), 82-88.
9. G. P. Celata, Heat transfer and fluid flow in microchannels, Begell House Inc., New York, 2004.
10. T.M Adams, M.F. Dowling, S.I. Abdel-Khalik, S.M. Jeter, Applicability of traditional turbulent single-phase forced convection correlations to non-circular microchannels, Int. J. of Heat and Mass Transfer 42 (1999), 4411-4415.
11. Z.-Y. Guo, Z.-X. Li, Size effect on single phase channel flow and heat transfer at microscale, Int. J. of Heat and Fluid Flow 24 (2003), 284-298.
12. G. L. Morini, Single-phase convective heat transfer in microchannels: a review of experimental results, Int. J. of Thermal Sciences 43 (2004), 631-651.
13. H. Herwig, O. Hausner, Critical view on “new results in micro-fluid mechanics”: an example, Int. J. of Heat and Mass Transfer 46 (2003), 935-937.
14. G. Hetsroni, A. Mosyak, E. Pogrebnyak, L.P. Yarin, Heat transfer in micro-channels: Comparison of experiments with theory and numerical results, Int. J. of Heat and Mass Transfer 48 (2005), 5580-5601.
15. N. T. Obot, Toward a better understanding of friction and heat/mass transfer in microchannels – A literature review, Microscale Thermophysical Engineering 6 (2002), 155-173.
16. B. Palm, Heat transfer in microchannels, Microscale Thermophysical Eng. 5 (2001), 155-175.
17. A. A. Rostami, A. S. Mujumdar, N. Saniei, Flow and heat transfer for gas flowing in microchannels: a review, Heat and Mass Transfer 38, 2002, 359-367.
18. G. L. Morini, Scaling effects for liquid flows in microchannels, Heat Transfer Engineering 27 (4) (2006), 64-73.
19. P. S. Lee, S. V. Garimella, D. Liu, Investigation of heat transfer in rectangular microchannels, Int. J. of Heat and Mass Transfer 48 (2005), 1688-1704.

20. P. Gao, S. Le Person, M. Favre-Marinet, Hydrodynamics and heat transfer in two-dimensional mini and microchannels, Int. J. of Heat and Mass Transfer 45 (2002), 1017-1027.
21. R.K. Shah, A.L. London, Advances in heat transfer. Supplement 1: laminar forced convection in ducts. New York: Academic Press; 1978.
22. A. Bucci, G. P. Celata, M. Cumo, E. Serra, G. Zummo, Water single-phase fluid flow and heat transfer in capillary tubes, Thermal Science and Engineering, Vol. 11, No. 6, (2003), 81-89.
23. H. Hausen, Neue Gleichungen für die Wärmeübertragung bei freier oder erzwungener Strömung, Allg. Waermetech, Vol. 9, (1959), pp. 75-79.
24. G. P. Celata, M. Cumo, V. Marconi, S. J. McPhail, G. Zummo, Microtube liquid single-phase heat transfer in laminar flow, Int. J. of Heat and Mass Transfer 49 (2006), 3538-3546.
25. R. Muwanga, I. Hassan, Local heat transfer measurements in microchannels using liquid crystal thermography: methodology development and validation, J. of Heat Transfer, Vol.128, (2006), 617-626.
26. D. Lelea, S. Nishio, K. Takano, The experimental research on microtube heat transfer and fluid flow of distilled water, Int. J. of Heat and Mass Transfer 47 (2004), 2817-2830
27. K. C. Toh, X. Y. Chen, J.C. Chai, Numerical computation of fluid flow and heat transfer in microchannels, Int. J. of Heat and Mass Transfer 45 (2002), 5133-5141.
28. H. Herwig, S. P. Mahulikar, Variable property effects in single-phase incompressible flows through microchannels, Int. J. of Thermal Sciences 45 (2006), 977-981.
29. M. Gad-el-Hak, The fluid mechanics of microdevices – The Freeman scholar lecture, Journal of Fluids Engineering, vol. 121 (1999) 5-33.
30. M. Von Smoluchowski, , Ueber Wärmeleitung in verdünnten gasen, Annalen der Physik und Chemie, Vol. 64 (1898) 101-130.
31. L. Ghodoossi, N. Eğrican, Prediction of heat transfer characteristics in rectangular microchannels for slip flow regime and H1 boundary condition, Int. J. of Thermal Sciences 44 (2005), 513-520.
32. S. Yu, T.A. Ameel, Slip-flow heat transfer in rectangular microchannels, Int. J. of Heat and Mass Transfer 44 (2001), 4225-4234.
33. G.A. Bird, Molecular Gas Dynamics and the Direct Simulation of Gas Flows, Clarendon Press, Oxford, United Kingdom, 1994.
34. M.D. Mikhailov, R.M. Cotta, Mixed symbolic-numerical computation of convective heat transfer with slip flow in microchannels, Int. Comm. in Heat and Mass Transfer 32 (2005), 341-348.
35. C.-H. Chen, Slip-flow heat transfer in a microchannel with viscous dissipation, Heat Mass Transfer 42 (2006), 853-860.
36. H.-E. Jeong, J.-T. Jeong, Extended Graetz problem including streamwise conduction and viscous dissipation in microchannel, Int. J. of Heat and Mass Transfer 49 (2006), 2151-2157.
37. B. Cao, G. W. Chen, Q. Yuan, Fully developed laminar flow and heat transfer in smooth trapezoidal microchannel, Int. Comm. In Heat and Mass Transfer 32 (2005), 1211-1220.

38. G. Tunc, Y. Bayazitoglu, Heat transfer in microtubes with viscous dissipation, Int. J. of Heat and Mass Transfer 44 (2001), 2395-2403.
39. R.S. Myong, D.A. Lockerby, J.M. Reese, The effect of gaseous slip on microscale heat transfer: An extended Graetz problem, Int. J. of Heat and Mass Transfer 49 (2006), 2502-2513.
40. R.S. Myong, J.M. Reese, R.W. Barber, D.R. Emerson, Velocity slip in microscale cylindrical Couette flow: the Langmuir model, Phys Fluids 17 (2005) 087105.
41. A. G. Fedorov, R. Viskanta, Three-dimensional conjugate heat transfer in the microchannel heat sink for electronic packaging, Int. J. of Heat and Mass Transfer 43 (2000), 399-415.
42. G. Gamrat, M. Facre-Marinet, D. Asendrych, Conduction and entrance effects on laminar liquid flow and heat transfer in rectangular microchannels, Int. J. of Heat and Mass Transfer 48 (2005), 2943-2954.
43. G. Maranzana, I. Perry, D. Maillet, Mini- and micro-channels: influence of axial conduction in the walls, Int. J. of Heat and Mass Transfer 47 (2004), 3993-4004.
44. J. Koo, C. Kleinstreuer, Viscous dissipation effects in microtubes and microchannels, Int. J. of Heat and Mass Transfer 47 (2004), 3159-3169.
45. J. Nikuradse, Strmunsgesetze in rauhen rohren, V.D.I. Forschungsheft 361 (1933) , 1-22.
46. L.F. Moody, Friction Factors for Pipe Flow, J. Heat Transfer, vol. 66, (1944), pp. 671-684.
47. G.M. Mala, D. Li, Flow characteristics of water in microtubes, Int. J. of Heat and Fluid Flow 20 (1999), 142-148.
48. J. Koo, C. Kleinstreuer, Analysis of surface roughness effects on heat transfer in micro-conduits, Int. J. of Heat and Mass Transfer 48 (2005),2625-2634.
49. G. Croce, P. D'Agaro, Numerical analysis of roughness effects on microtube heat transfer, Superlattices and Microstructures 35 (2004), 601-616.
50. G. Croce, P. D'Agaro, Numerical simulation of roughness effect on microchannel heat transfer and pressure drop in laminar flow, J. Phys. D: Appl. Phys. 38 (2005), 1518-1530.
51. Y. Ji, K. Yuan, J. N. Chung, Numerical simulation of wall roughness on gaseous flow and heat transfer in a microchannel, Int. J. of Heat and Mass Transfer 49 (2006), pp. 1329-1339.
52. S. Shen, J. L. Xu, J. J. Zhou, Y. Chen, Flow and heat transfer in microchannels with rough wall surface, Energy Conversion and Management 47 (2006), 1311-1325.
53. H. Y. Wu, Ping Cheng, An experimental study of convective heat transfer in silicon microchannels with different surface conditions, Int. J. of Heat and Mass Transfer 46 (2003), 2547-2556.
54. G. M. Mala, D. Li, J. D. Dale, Heat transfer and fluid flow in microchannels, Int. J. Heat and Mass Transfer, Vol. 40, No. 13 (1997), 3079-3088.
55. E. Y. K. Ng, S. T. Tan, Computation of three-dimensional developing pressure-driven liquid flow in a microchannel with EDL effect, Numerical Heat Transfer, Part A, 45 (2004), 1013-1027.
56. S. T. Tan, E. Y. K. Ng, Numerical analysis of EDL effect on heat transfer characteristic of 3-D developing flow in a microchannel, Numerical Heat Transfer, Part A, 49, (2006) 991-1007.

57. V. Gnielinski, New equations for heat transfer in turbulent pipe and channel flow, International Chemical Engineering, Vol. 16 (1976), 359-368, 1976.
58. W. Owhaib, B. Palm, Experimental investigation of single-phase convective heat transfer in circular microchannels, Experimental Thermal and Fluid Science 28 (2004), 105-110.
59. R. Bavière, M. Favre-Marinet, S. Le Person, Bias effects on heat transfer measurements in microchannel flows, Int. J. of Heat and Mass Transfer 49 (2006), 3325-3337.
60. A. Bejan, A.D. Kraus, Heat Transfer Handbook, John Wiley & Sons, Inc., Hoboken, New Jersey, 2003.
61. F. W. Dittus, L.M.K. Boelter, Heat transfer in automobile radiators of tubular type, Univ. California, Berkeley, Publ. Eng. 2 (13) (1930), 443-461.
62. B. Petukhov, V. Kurgano, A. Gladuntsov, Heat transfer in turbulent pipe flow of gases with variable properties, Heat Transfer Sov. Res. 5 (1973), 109-116.
63. S. B. Choi, R.F. Barron, R. O. Warrington, Fluid flow and heat transfer in microtubes. Micromechanical Sensors, Actuators and Systems, ASME DSC 32, pp. 123-134, Atlanta, GA, 1991.
64. D. Yu, R. O. Warrington, R. Barron, T. Ameel, An experimental and theoretical investigation of fluid flow and heat transfer in microtubes. Proceedings of ASME/JSME Thermal Engineering Joint Conf., pp. 523-530, Maui, HI, 1995.
65. O. Tonomura, S. Tanaka, M. Noda, M. Kano, S. Hasebe, I. Hashimoto, CFD-based optimal design of manifold in plate-fin microdevices, Chem. Eng. Journal 101 (2004), 397-402.
66. W.J. Duncan, A.S. Thom, A.D. Young, Mechanics of Fluids, 2nd Ed., Arnold, 1970.
67. S. Haas, Lattice Boltzmann Fluid Dynamics, http://rzlnx5.mpie-duesseldorf.mpg.de/1208/, 16.12.2005.
68. Hudong Chen et al., Extended Boltzmann Kinetic Equation for Turbulent Flows, Science, 301, 633-636, 1 August 2003.
69. H. Xue, H. Ji, C. Shu, Prediction of Flow and Heat Transfer Characteristics in Micro Couette Flows, Microscale Thermophysical Engineering 7 (2003) 51-68.
70. J.M. Buick et al., The Lattice Boltzmann Equation for Modelling Arterial Flows: Review and Application, Internal Medicine, II, (2003) 24-29.
71. S. Chapman, On the law of distribution of velocities and on the theory of viscosity and thermal conduction in a non-uniform, simple, monatomic gas, Phil. Trans. Royal Soc. A 216, (1916) 279
72. D. Enskog, The kinetic theory of phenomena in fairly rare gases, Dissertation, Upsala, 1917.
73. P.L. Bhatnagar, E.P. Gross, Krook, M., A Model for Collision Processes in Gases. I. Small Amplitude Processes in Charged and Neutral One-Component Systems, Phys Rev 94 (1954) 511-524.
74. F. Galbusera, M Cioffi, M.T. Raimondi, R. Pietrabissa, Computational modelling of combined cell population, dynamics and oxygen transport in engineered tissue subject to interstitial perfusion, Comp. Meth. in Biomech & Biomed Eng 10 (4) (2007), 279-287.

Figure captions

Fig.1: Channel length *L* above which entrance effects can be neglected as a function of the Reynolds number and with the hydraulic diameter as a parameter ($Pr = 5.5$).

Fig. 2: Effect of temperature dependent fluid properties on the Nusselt number (from Herwig and Mahulikar [28])

Fig. 3: Variation of the Nusselt number with $\beta = \beta_t / \beta_v$, for a rectangular microchannel (from Ghodoossi and Egrican [31])

Fig. 4: Compressibility effects (from Guo and Li [11]). A: Radial temperature profiles at different axial locations with (full lines) and without (dashed lines) compressibility effects; B: Nusselt number for compressible flows with different inlet Mach number

Fig. 5: Different competing scaling effects (from Morini [18])

Fig. 6: Effect of Brinkmann number on local Nusselt number (from Jeong and Jeong [36]). A: flow with constant wall temperature; B: flow with constant wall heat flux

Fig. 7: Viscous heating effects (from Chen [35]). A: Effects of rarefaction and viscous heating on the local Nusselt number; B: Effects of the Brinkmann number on the local Nusselt number for rarefied flows

Fig. 8: Nomenclature for the trapezoidal cross section used by Wu and Cheng [53]

Fig. 9: Surface roughness effects on the average Nusselt number

Fig. 10: Electric Double Layer (from Mala et al. [54])

Fig. 11: Sketch of the test section considered in [20], [42] and [59] (from Gao et al. [20])

Fig. 12: Cross-section geometry of the unit cell in Shen et al. [52]

Fig. 13: Comparison of correlations. A: laminar flows in circular channels; B: turbulent flows

Fig. 14: Knudsen number regimes (after Gad-el-Hak [29])

Fig. 15: Overall relationships of models in fluid dynamics (adapted from Gad-el-Hak [29])

Table 1. Graetz number ranges in the examined papers.

Reference	Gz range	Entrance Effects (Y/N)
Lee et al. [19]	Gz = 20-400	YES
Gao et al. [20]	Gz = 22-3000	YES
Bucci et al. [22]	Gz = 1.5-160	YES
Celata et al. [24]	Gz = 6-233	YES
Muwanga and Hassan [25]	Gz = 35-290	YES
Lelea et al. [26]	Gz = 0.05-250	YES

Table 2. Summary of experimental results. A: single microchannels; B: parallel microchannels

A) EXPERIMENTS WITH SINGLE MICROCHANNELS				
Reference	**Cross section**	**d_h [μm]**	***Re***	**Heat transfer behaviour**
Bucci et al. [22]	Circular	172-520	200-6000	$Nu < Nu_{pr}$ laminar flow $Nu \approx Nu_{pr}$ turbulent flow
Owhaib and Palm [58]	Circular	800-1700	1000-17000	$Nu \approx Nu_{pr}$
Gao et al. [20]	Rectangular (2D)	200-2000	100-8000	$Nu \approx Nu_{pr}$ $Nu < Nu_{pr}$ for $d_h < 1000\ \mu m$
Bavière et al [59]	Rectangular (2D)	200-700	100-8000	$Nu \approx Nu_{pr}$
Celata et al. [24]	Circular	50-528	50-2775	$Nu \approx Nu_{pr}$ $Nu < Nu_{pr}$ for the lowest diameters
Muwanga and Hassan [25]	Circular	1066	600-5000	$Nu \approx Nu_{pr}$
Lelea et al. [26]	Circular	125-500	100-800	$Nu \approx Nu_{pr}$ Moreover, experimental results are in good agreement with numerical simulations with temperature dependent properties.

B) EXPERIMENTS WITH PARALLEL MICROCHANNELS				
Reference	**Cross section**	**d_h [μm]**	***Re***	**Heat transfer behaviour**
Lee et al. [19]	Rectangular	318-903	300-3500	The measured Nusselts numbers disagree both with standard and with microchannel correlations
Shen et al. [52]	Rectangular	436	162-1257	$Nu < Nu_{pr}$
Wu and Cheng [53]	Trapezoidal	135-320	10-1500	No comparisons

Table 3. Correlations for the average Nusselt number. A: thermally developing laminar flows in circular channels; B: turbulent flows; C: flows in microchannels

A: correlations for thermally developing laminar flows in circular channels

Reference	Boundary condition	Correlation	eq.
Hausen [23]	CWT	$Nu = 3.66 + \dfrac{0.19\left(RePrd/L\right)^{0.8}}{1+0.017\left(RePrd/L\right)^{0.467}}$	(20)
Hausen [23]	CWHF	$Nu = 4.36 + \dfrac{0.023\,RePrd/L}{1+0.012\,RePrd/L}$	(21)
Shah and London [21]	CWT	$Nu = 1.615(RePrd_h/L)^{1/3} - 0.70 \qquad RePrd_h/L \geq 200$ $Nu = 1.615(RePrd_h/L)^{1/3} - 0.20 \qquad 33.3 \leq RePrd_h/L \leq 200$ $Nu = 3.657 + 0.0499 RePrd_h/L \qquad RePrd_h/L < 33.3$	(22)
Shah and London [21]	CWHF	$Nu = 1.953\left(RePrd_h/L\right)^{1/3} \qquad RePrd/x \geq 33.3$ $Nu = 4.364 + 0.0722\,RePrd_h/L \qquad RePrd/x < 33.3$	(23)

B: correlations for turbulent flows

Reference	Boundary condition	Correlation	eq.
Gnielinski [57]	CWT	$Nu = \dfrac{(f/8)(Re-1000)Pr}{1+12.7(f/8)^{0.5}\left(Pr^{2/3}-1\right)}\left[1+\left(\dfrac{d}{L}\right)^{2/3}\right]$ $f = (1.82\log Re - 1.64)^{-2}$	(24)
Gnielinski [57]	CWHF	$Nu = \dfrac{(f/8)(Re-1000)Pr}{1+12.7(f/8)^{0.5}\left(Pr^{2/3}-1\right)}$ $f = (1.82\log Re - 1.64)^{-2}$	(25)
Dittus and Boelter [61]	CWHF	$Nu = 0.023 Re^{0.8} Pr^{0.4} \qquad Re > 10000$	(26)
Pethukov et al. [62]	CWHF	$Nu = \dfrac{(f/8)RePr}{R+12.7(f/8)^{1/2}\left(Pr^{2/3}-1\right)}$ $R = 1.07 + \dfrac{900}{Re} - \dfrac{0.63}{(1+10Pr)} \qquad Re > 10000$	(27)

C: correlations for flow in microchannels

Reference	Flow regime	Correlation	eq.
Choi et al. [63]	laminar, circular channels	$Nu = 0.000972 Re^{1.17} Pr^{1/3} \qquad Re < 2000$	(28)
Choi et al. [63]	turbulent	$Nu = 3.82\cdot 10^{-6} Re^{1.96} Pr^{1/3} \qquad 2500 < Re < 20000$	(29)
Yu et al. [64]	turbulent	$Nu = 0.007 Re^{1.2} Pr^{0.2} \qquad 6000 < Re < 20000$	(30)
Adams et al. [10]	turbulent	$Nu = Nu_{Gnielinski}(1+F)$ $F = 7.6\cdot 10^{-6} Re[1-(d_h/d_0)^2] \qquad d_0 = 1.164\ mm$	(31)

Table 4: Scaling effects and criteria for negligibility in microchannels

Scaling effect	Criterion	Comments
Rarefaction effects (only gas flows)	$Kn < 10^{-3}$ (ref. [29])	
Compressibility effects (only gas flows)		check the Mach number at the outlet of the flow
Temperature-dependent properties		check the properties variations between inlet and outlet, depending on the fluid temperature variations
Conjugate heat transfer	$M < 0.01$ (ref. [43])	
Viscous heating	$Br < \dfrac{\xi_{\lim} d_h^2}{2AfRe}$ (ref. [18])	
Surface roughness		Do not perform any corrections
EDL	$K > K_{\lim}$	

Table 5. Recommended models for *Kn* regimes. Gas flows: after Gad-el-Hak [29]; Liquid flows: abbreviated ranges after Haas [67]

GAS FLOWS			
***Kn* range**	**Range description**	**Recommended models**	**References**
$\rightarrow 0$	Neglect of diffusion	Euler equations	[29], 8, 2 & 10, 1
$\leq 10^{-3}$	Continuum (no slip)	Navier-Stokes equation	[29], 9/10
$10^{-3} \leq Kn \leq 10^{-1}$	Continuum with slip	Burnett equations	[69]
$10^{-1} \leq Kn \leq 10$	Transition to molecular flow	Direct Simulation Monte Carlo	[69], 2 Summary [29], 17, 2
$Kn > 10$	Free-molecule flow	Lattice Boltzmann	[29], 30, 1
Kn very large	Extreme range	Molecular Dynamics	[29], 15, 1
LIQUID FLOWS			
***Kn* range**	**Range description**	**Recommended models**	**References**
$Kn \leq 10^{-1}$	Continuum	Navier-Stokes equations	[67] fig. 3
$Kn \geq 10^{-1}$	Sub-continuum or molecular	Molecular	[67] fig. 3
Kn very large	Extreme range	Molecular Dynamics	[29], 15, 1

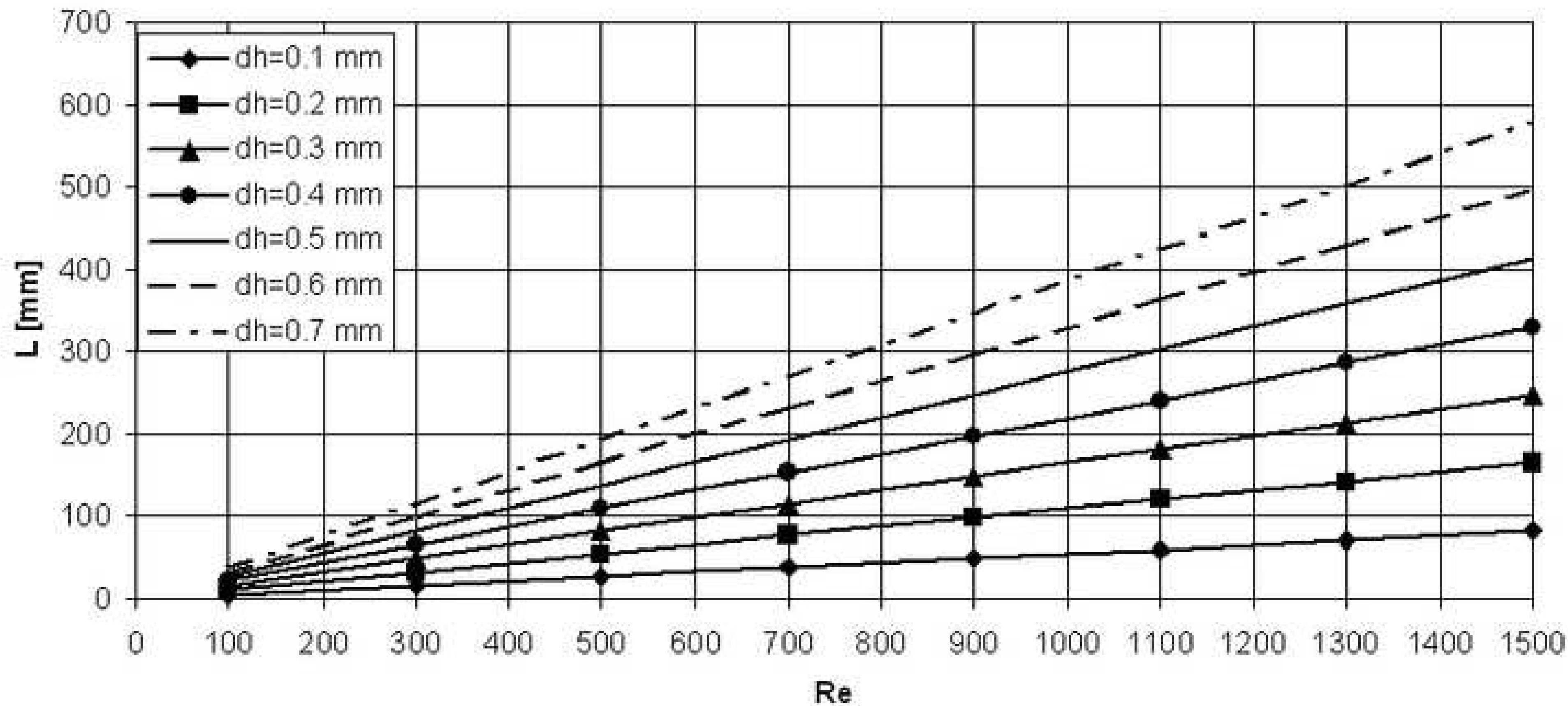

700
600
500
400
300
200
100
0
L [mm]
dh=0.1 mm
dh=0.2 mm
dh=0.3 mm
dh=0.4 mm
dh=0.5 mm
dh=0.6 mm
dh=0.7 mm
0
100
200
300
400
500
600
700
800
900
1000
1100
1200
1300
1400
1500
Re

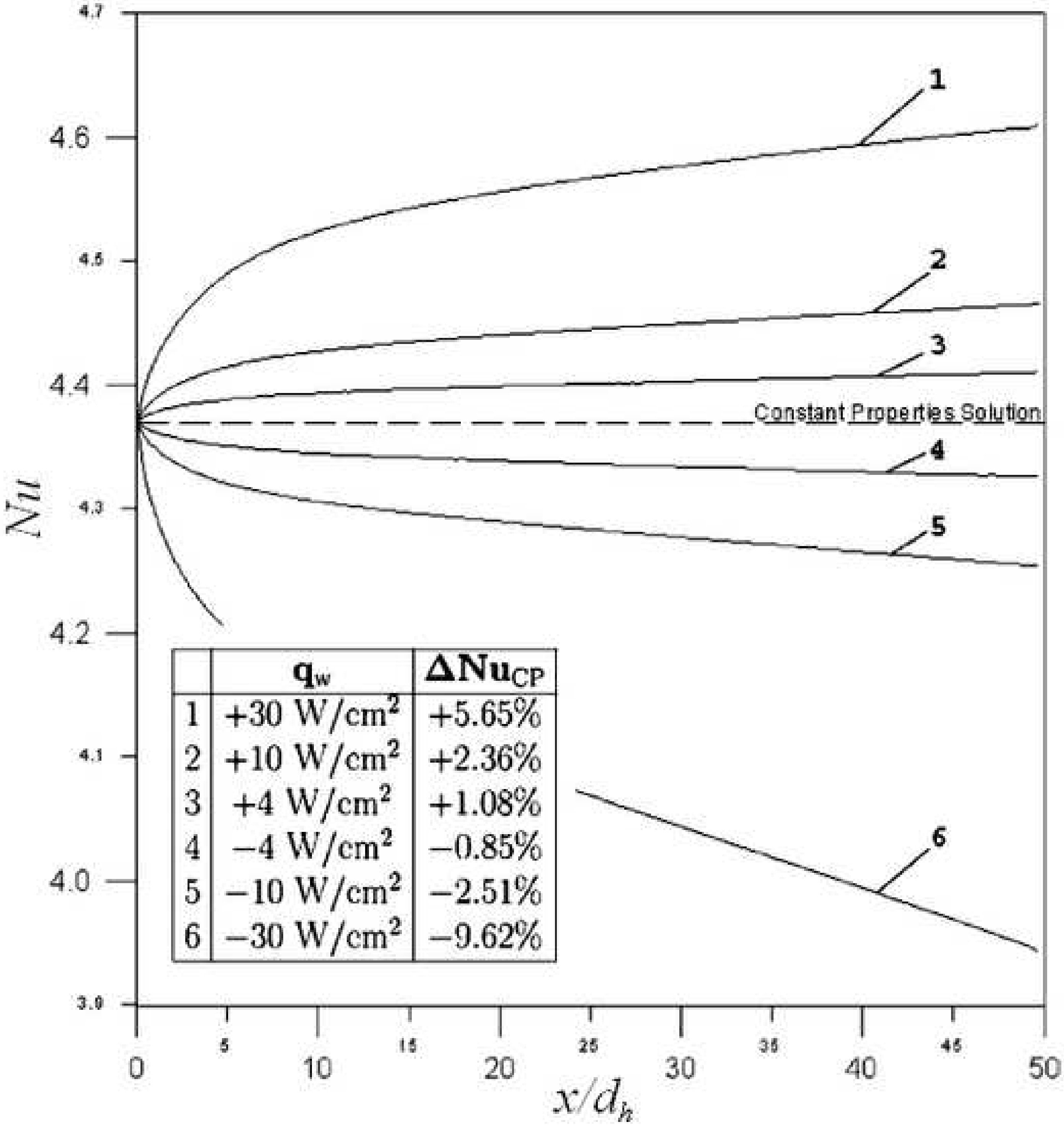
Nu
4.7
4.6
4.5
4.4
4.3
4.2
4.1
4.0
3.9
0
5
10
15
20
25
30
35
40
45
50
x/d_h
1
2
3
Constant Properties Solution
4
5
6
	q_w	ΔNu_{CP}
1	$+30$ W/cm^2	$+5.65\%$
2	$+10$ W/cm^2	$+2.36\%$
3	$+4$ W/cm^2	$+1.08\%$
4	-4 W/cm^2	-0.85%
5	-10 W/cm^2	-2.51%
6	-30 W/cm^2	-9.62%

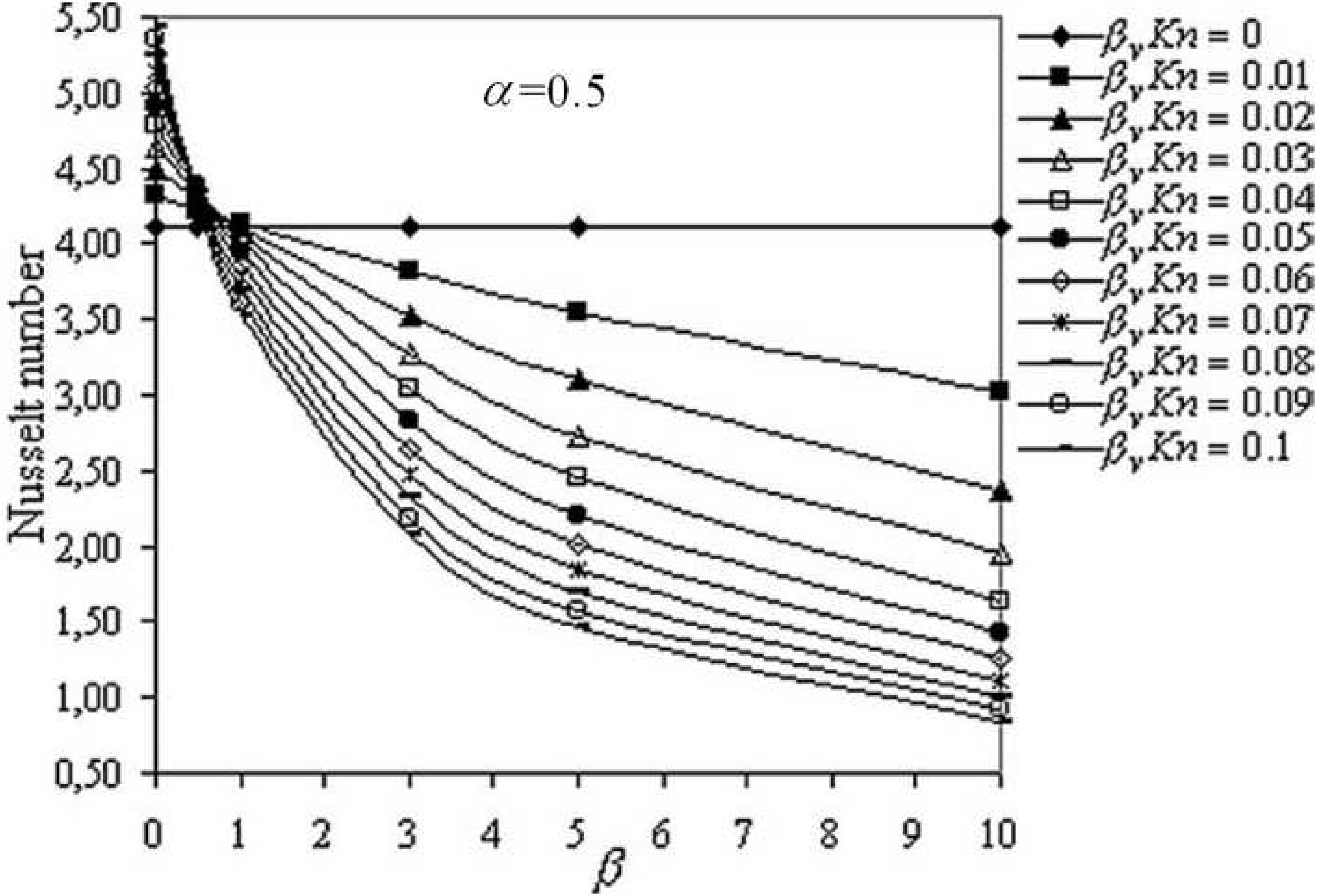

5,50
5,00
4,50
4,00
3,50
3,00
2,50
2,00
1,50
1,00
0,50
Nusselt number
0
1
2
3
4
5
6
7
8
9
10
β
α=0.5
$\beta_v Kn = 0$
$\beta_v Kn = 0.01$
$\beta_v Kn = 0.02$
$\beta_v Kn = 0.03$
$\beta_v Kn = 0.04$
$\beta_v Kn = 0.05$
$\beta_v Kn = 0.06$
$\beta_v Kn = 0.07$
$\beta_v Kn = 0.08$
$\beta_v Kn = 0.09$
$\beta_v Kn = 0.1$

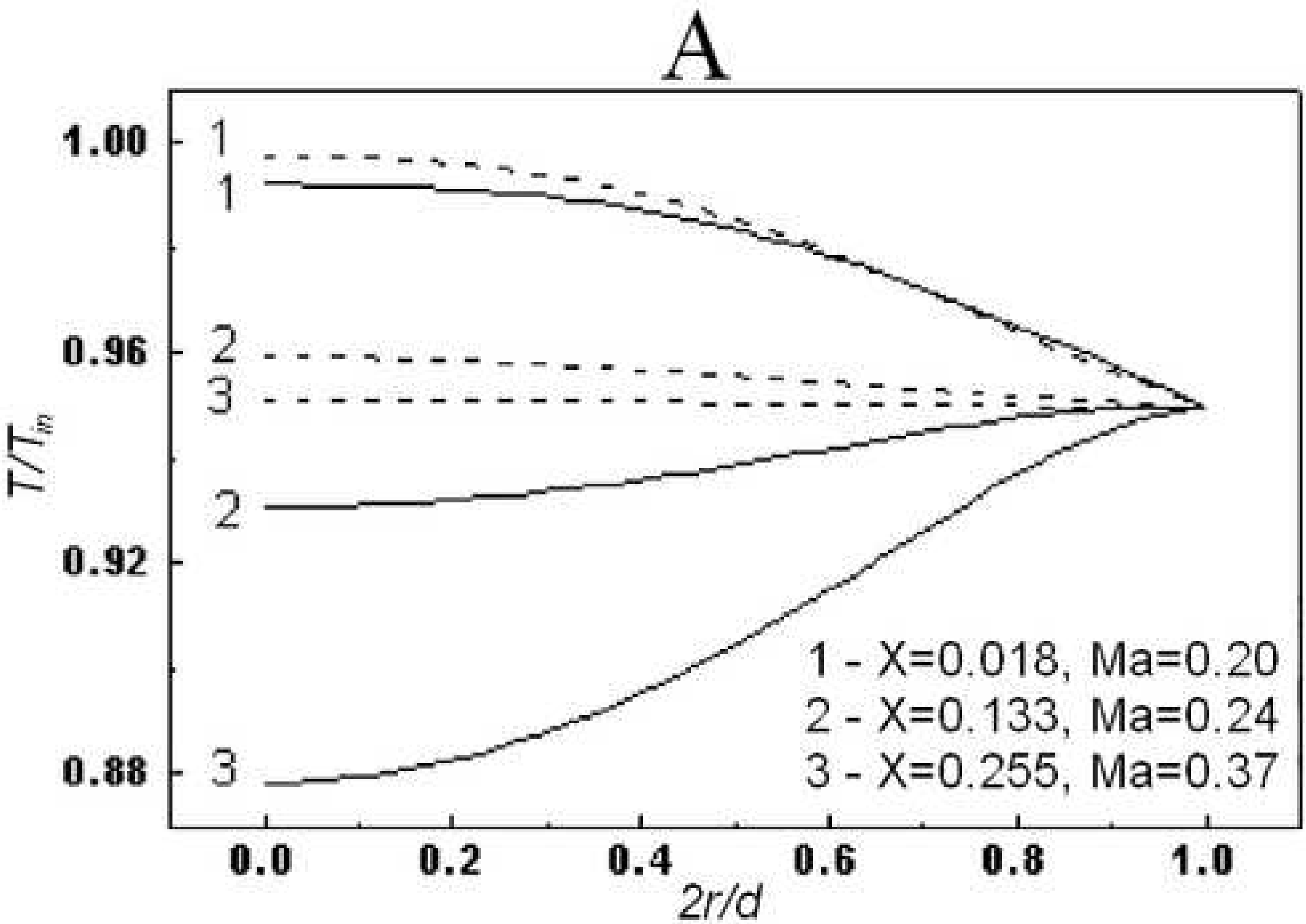
A
1.00
0.96
0.92
0.88
T/T_in
1
1
2
3
2
3
1 - X=0.018, Ma=0.20
2 - X=0.133, Ma=0.24
3 - X=0.255, Ma=0.37
0.0
0.2
0.4
0.6
0.8
1.0
2r/d

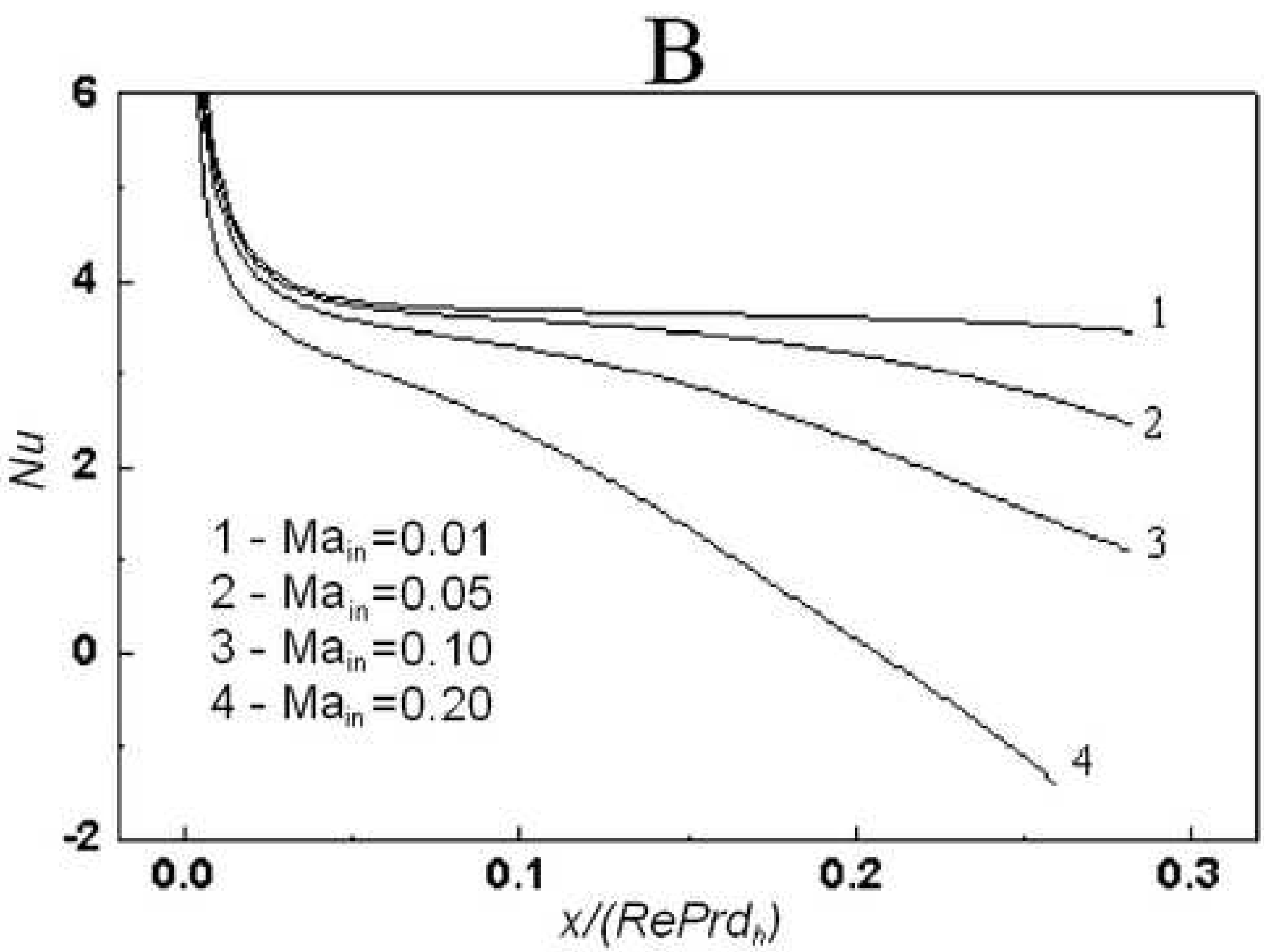
B
6
4
2
0
-2
Nu
1
2
3
4
1 - Ma_in=0.01
2 - Ma_in=0.05
3 - Ma_in=0.10
4 - Ma_in=0.20
0.0
0.1
0.2
0.3
x/(RePrd_h)

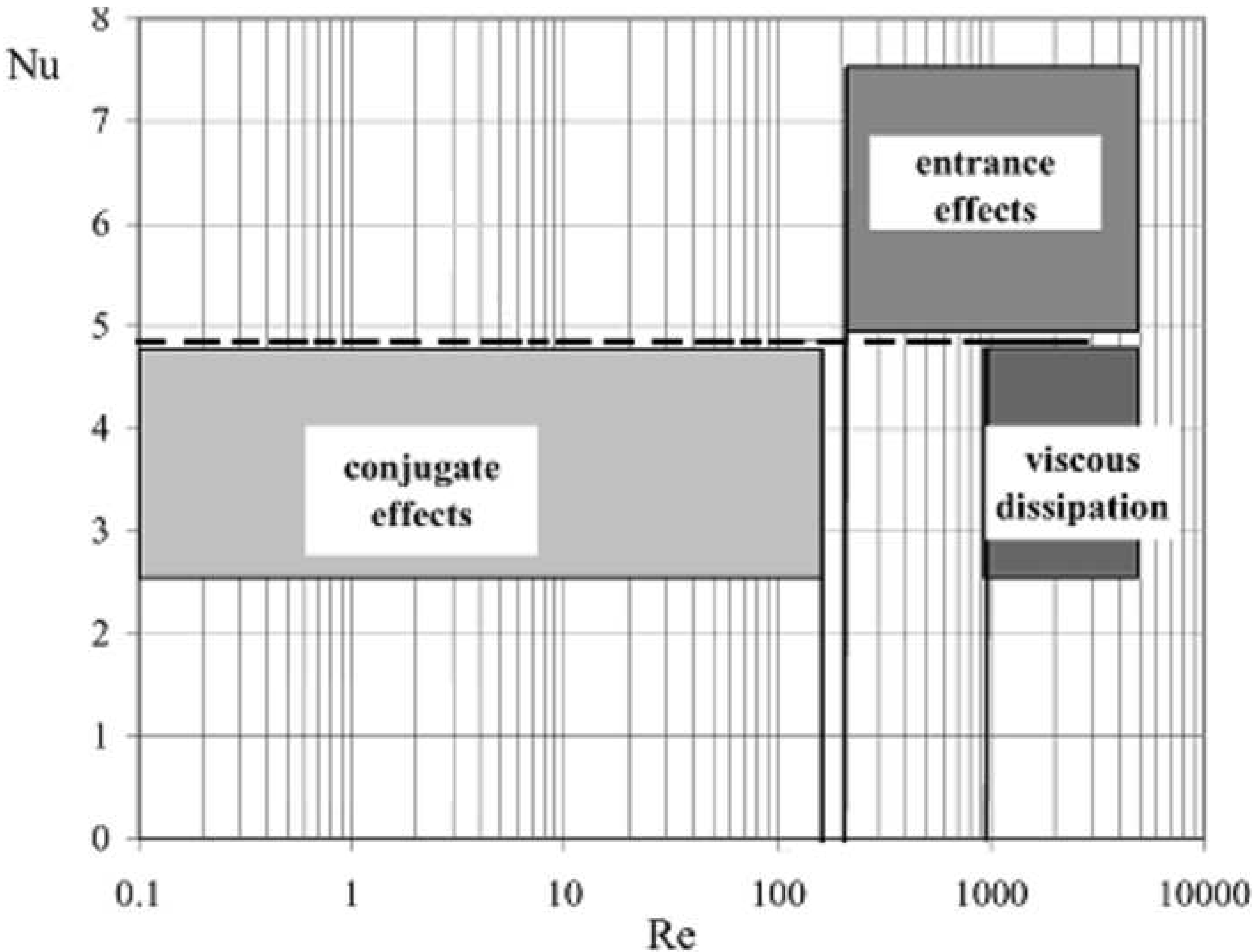

Nu
8
7
6
5
4
3
2
1
0
0.1
1
10
100
1000
10000
Re
entrance effects
conjugate effects
viscous dissipation

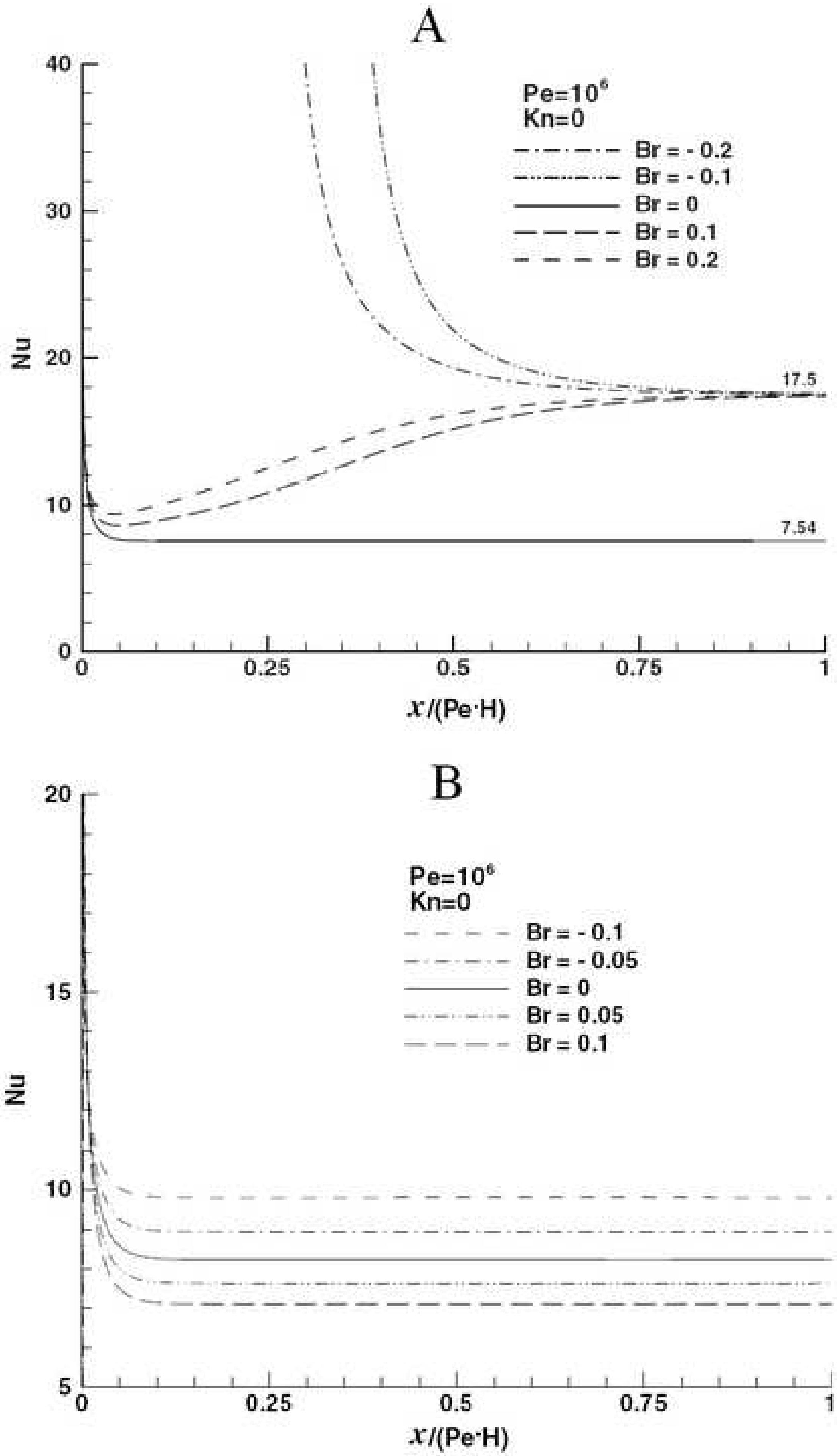

A
Pe=10⁶
Kn=0
Br = - 0.2
Br = - 0.1
Br = 0
Br = 0.1
Br = 0.2
Nu
17.5
7.54
x/(Pe·H)
B
Pe=10⁶
Kn=0
Br = - 0.1
Br = - 0.05
Br = 0
Br = 0.05
Br = 0.1
Nu
x/(Pe·H)

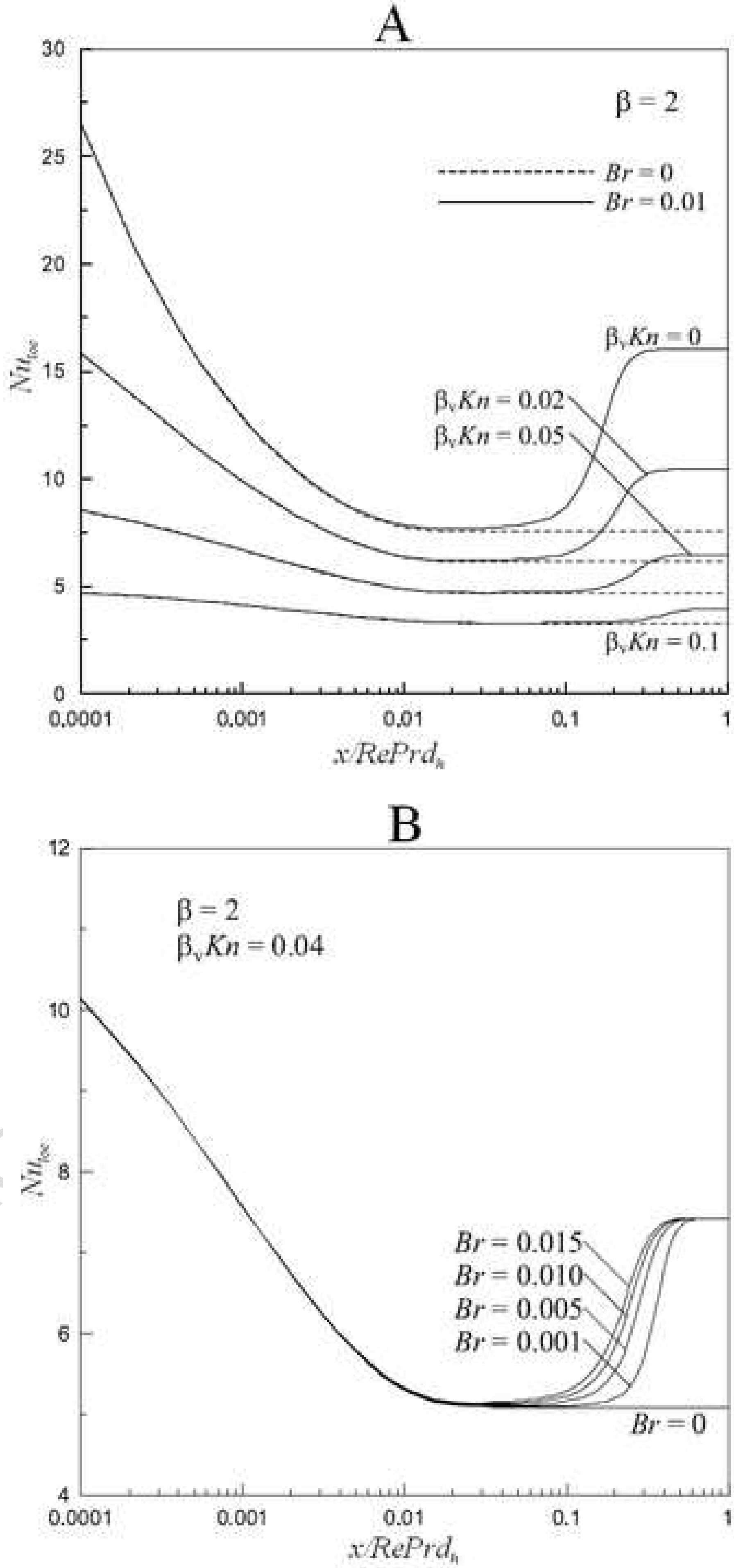
A
β = 2
Br = 0
Br = 0.01
βvKn = 0
βvKn = 0.02
βvKn = 0.05
βvKn = 0.1
Nuloc
x/RePrdh
B
β = 2
βvKn = 0.04
Br = 0.015
Br = 0.010
Br = 0.005
Br = 0.001
Br = 0
Nuloc
x/RePrdh

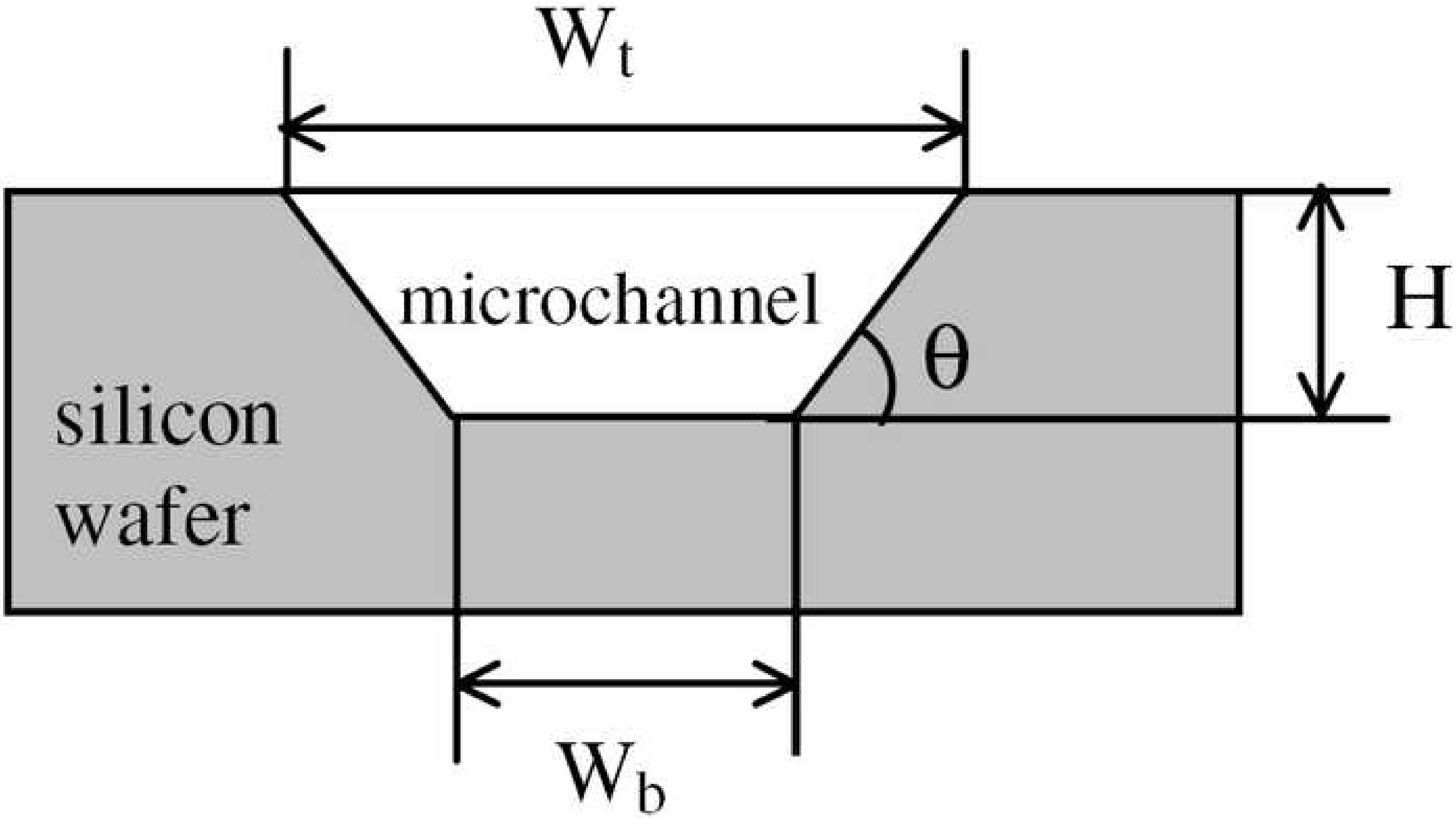

W_t
microchannel
θ
H
silicon
wafer
W_b

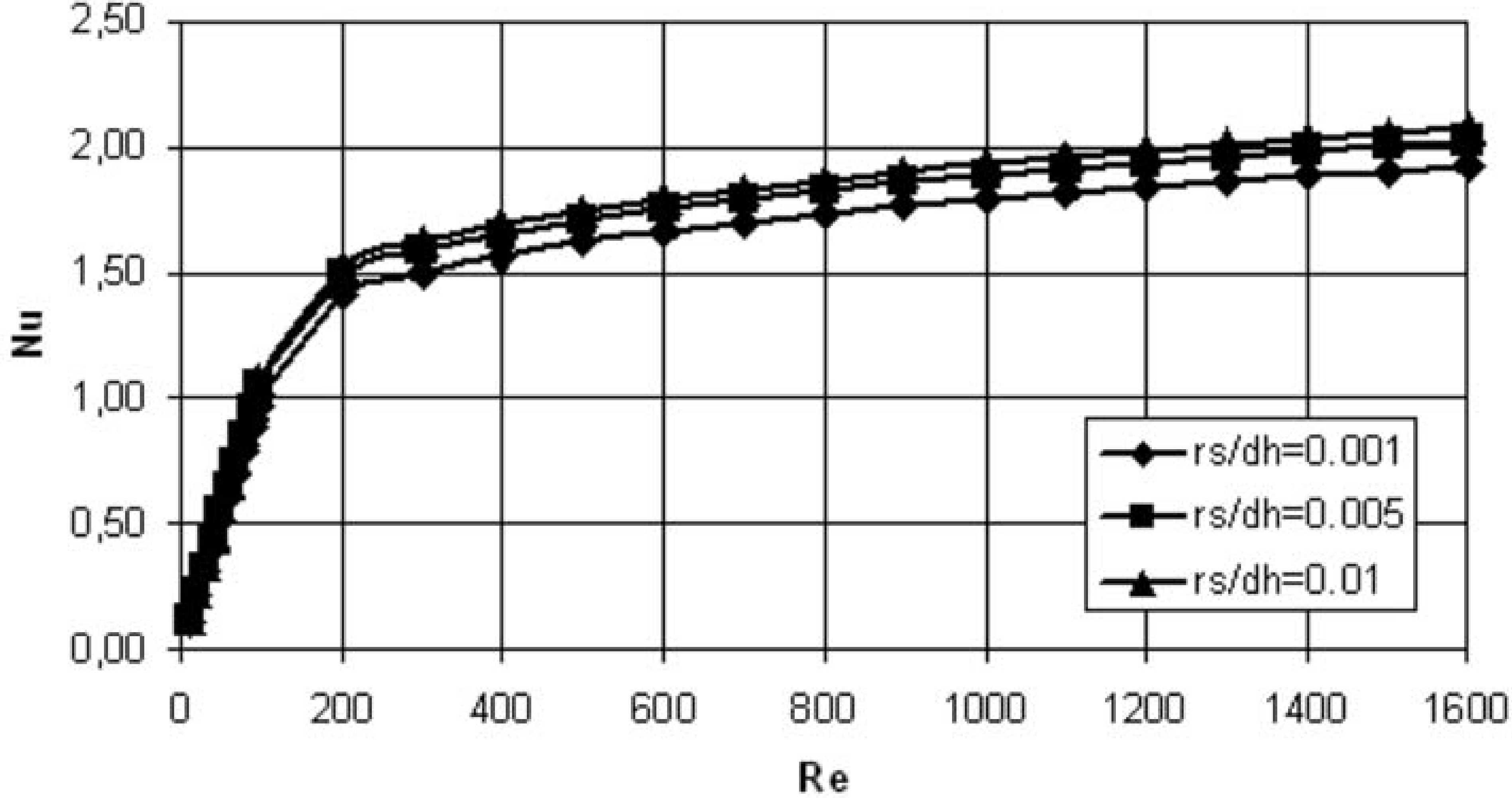
2,50
2,00
1,50
1,00
0,50
0,00
Nu
0
200
400
600
800
1000
1200
1400
1600
Re
rs/dh=0.001
rs/dh=0.005
rs/dh=0.01

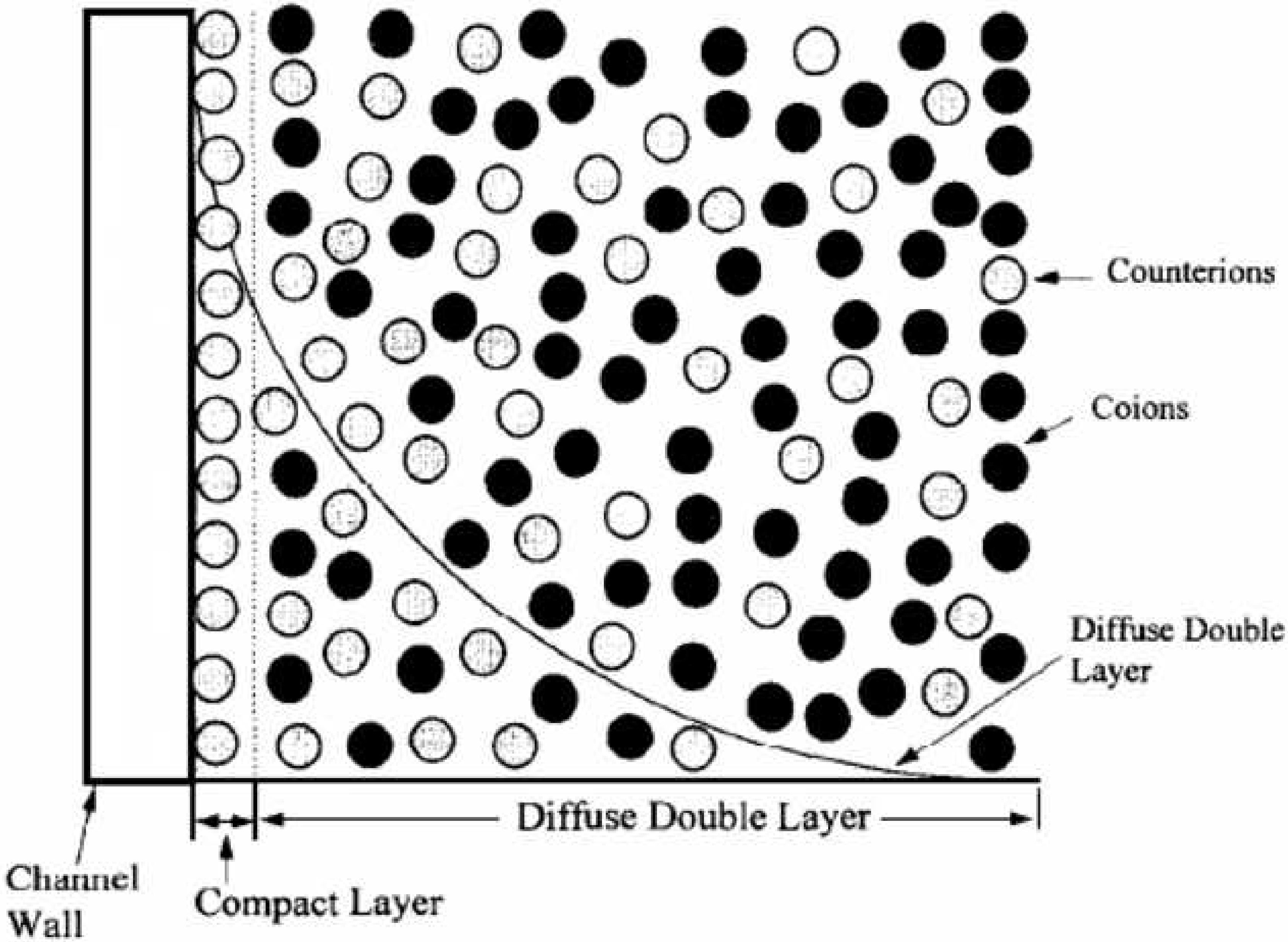
Counterions
Coions
Diffuse Double Layer
Diffuse Double Layer
Channel Wall
Compact Layer

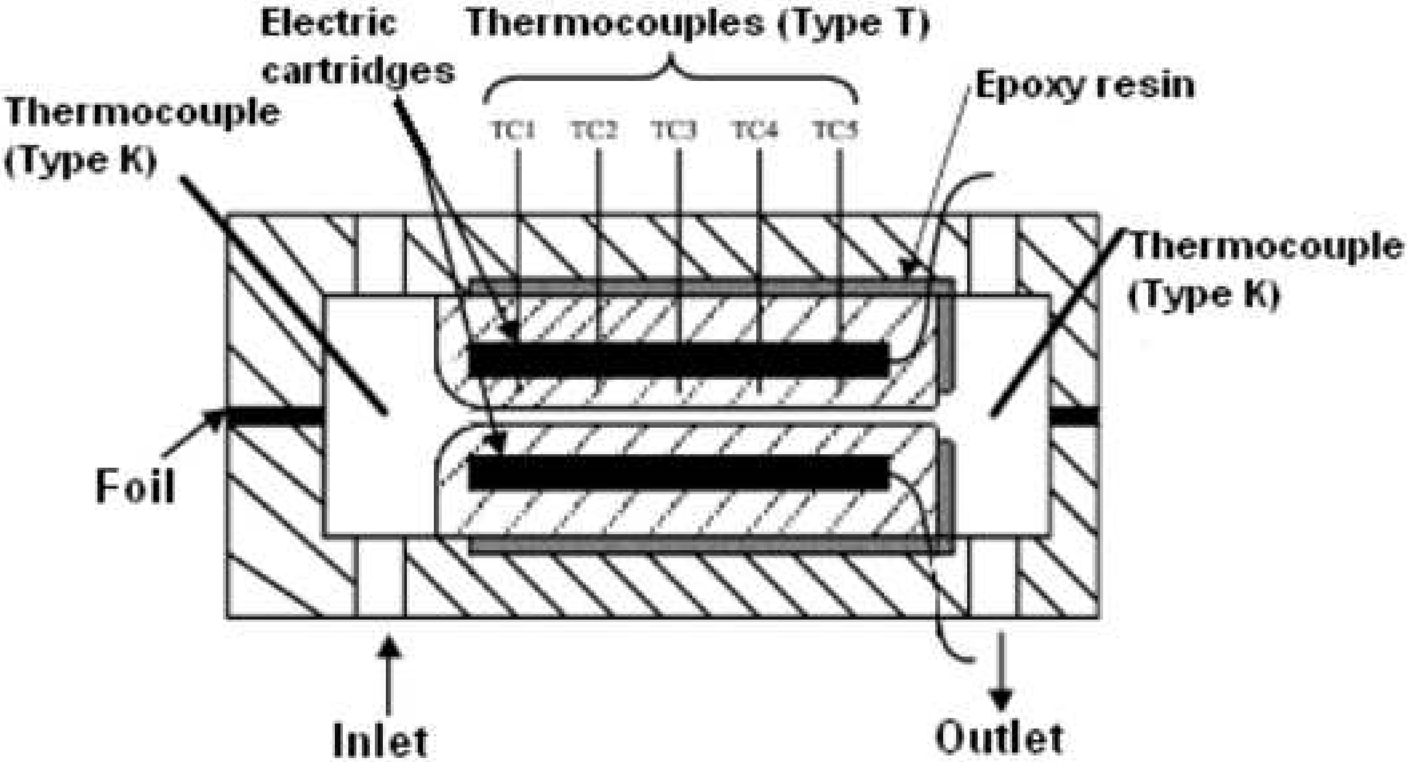
Electric cartridges
Thermocouples (Type T)
TC1
TC2
TC3
TC4
TC5
Epoxy resin
Thermocouple (Type K)
Thermocouple (Type K)
Foil
Inlet
Outlet

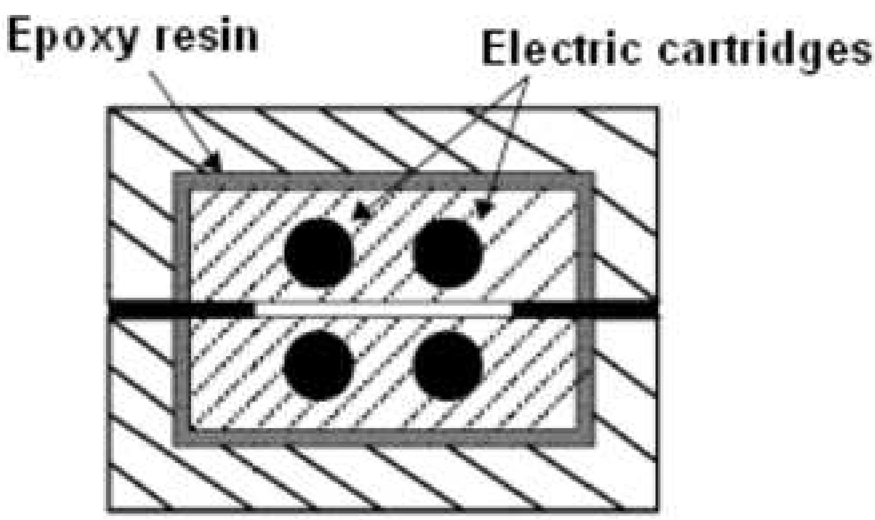
Epoxy resin
Electric cartridges

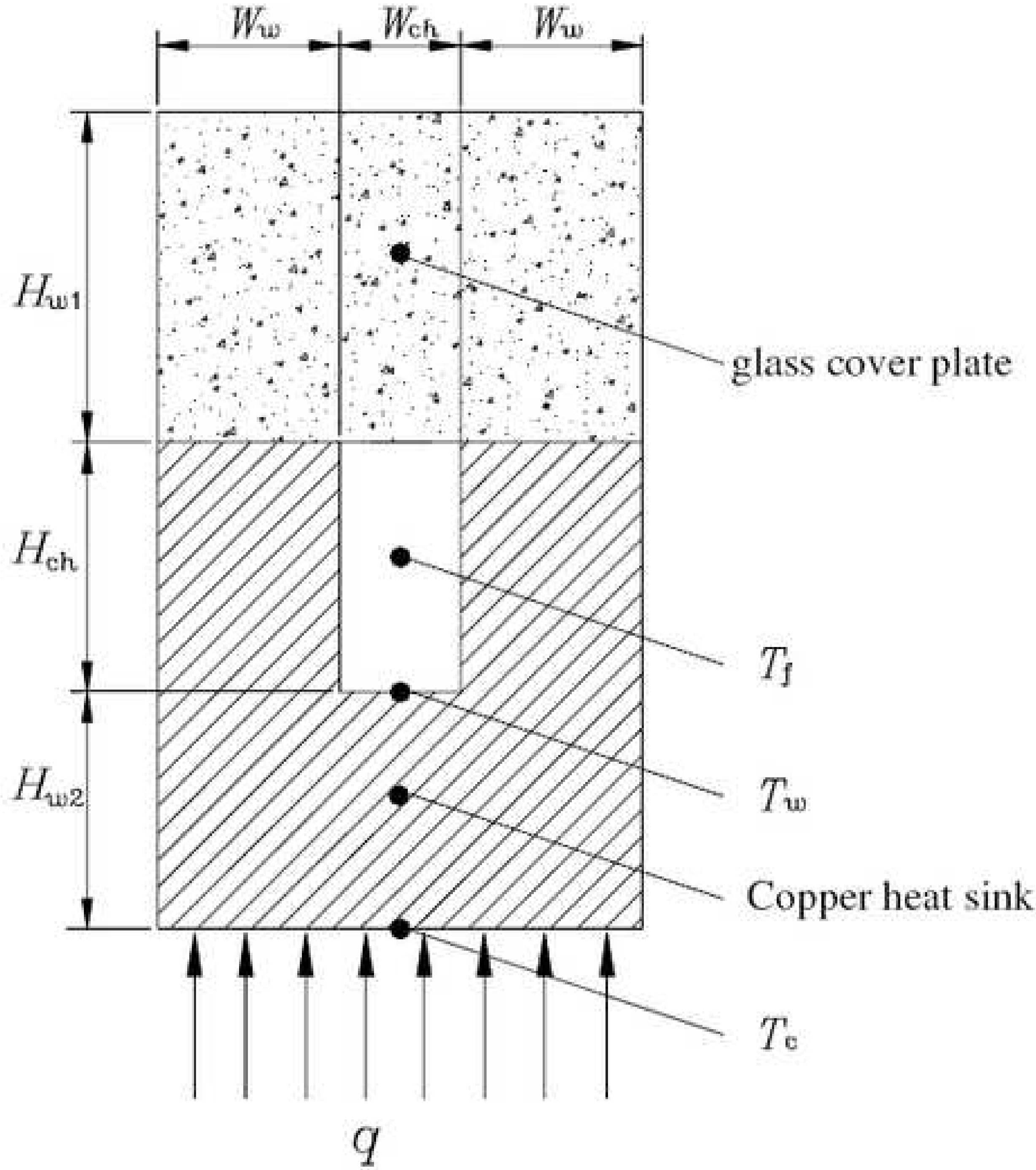

W_w (μm)	W_{ch} (μm)	H_{w1} (μm)	H_{ch} (μm)	H_{w2} (μm)
150	300	5000	800	6200

A

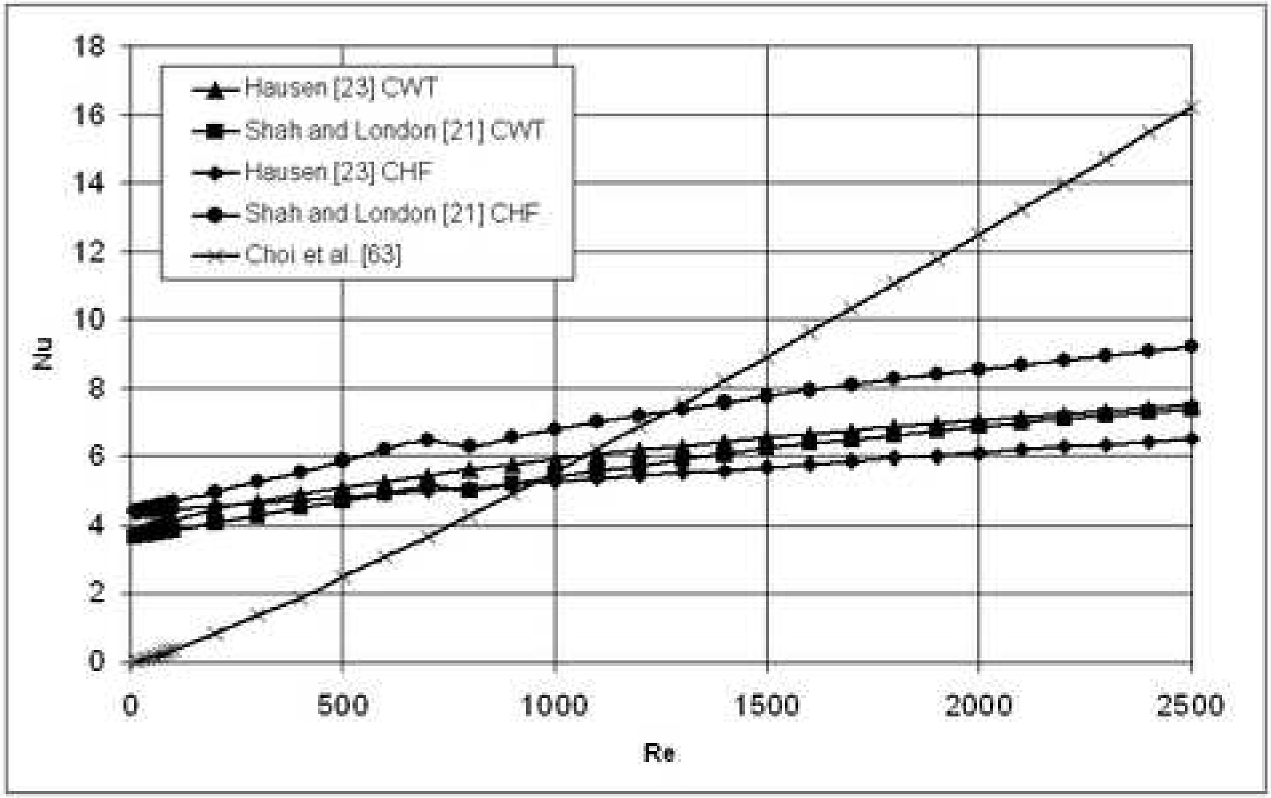

Hausen [23] CWT
Shah and London [21] CWT
Hausen [23] CHF
Shah and London [21] CHF
Choi et al. [63]
Nu
Re
0
2
4
6
8
10
12
14
16
18
0
500
1000
1500
2000
2500

B

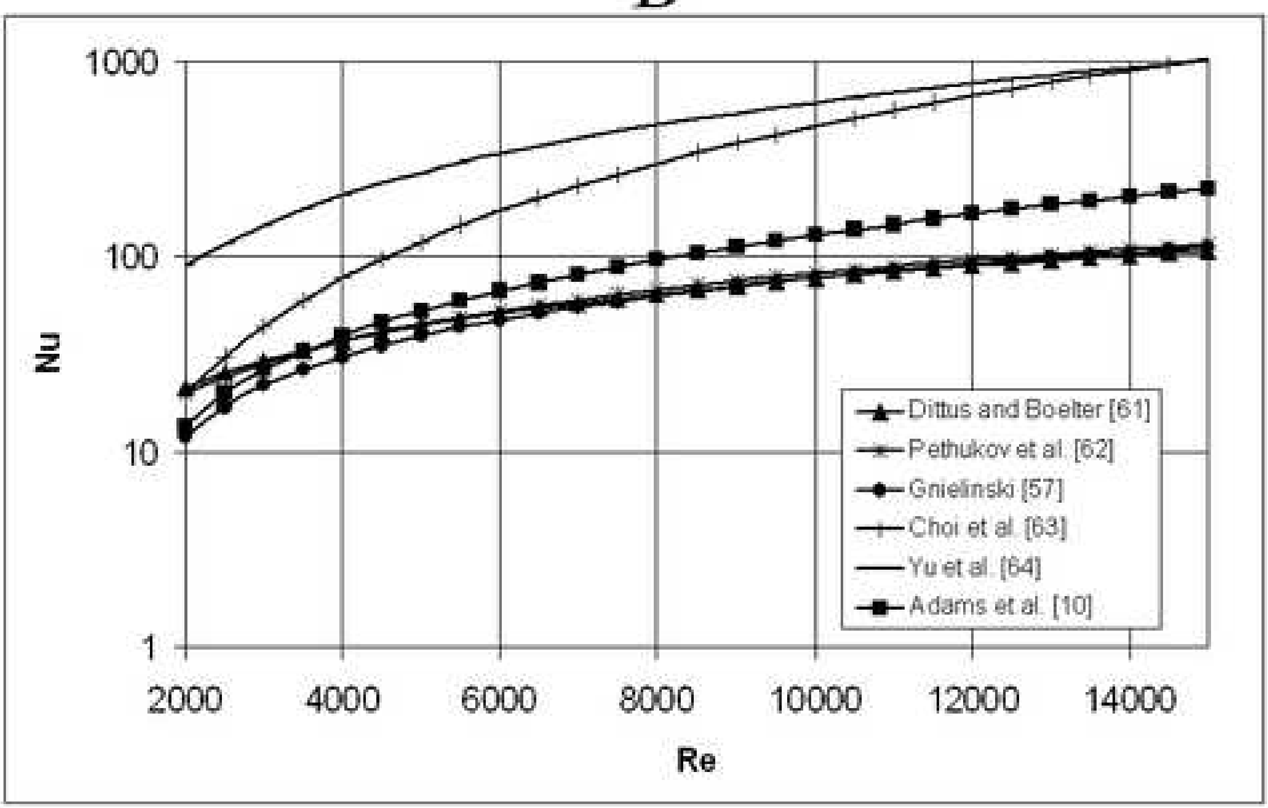

Dittus and Boelter [61]
Pethukov et al. [62]
Gnielinski [57]
Choi et al. [63]
Yu et al. [64]
Adams et al. [10]
Nu
Re
1
10
100
1000
2000
4000
6000
8000
10000
12000
14000

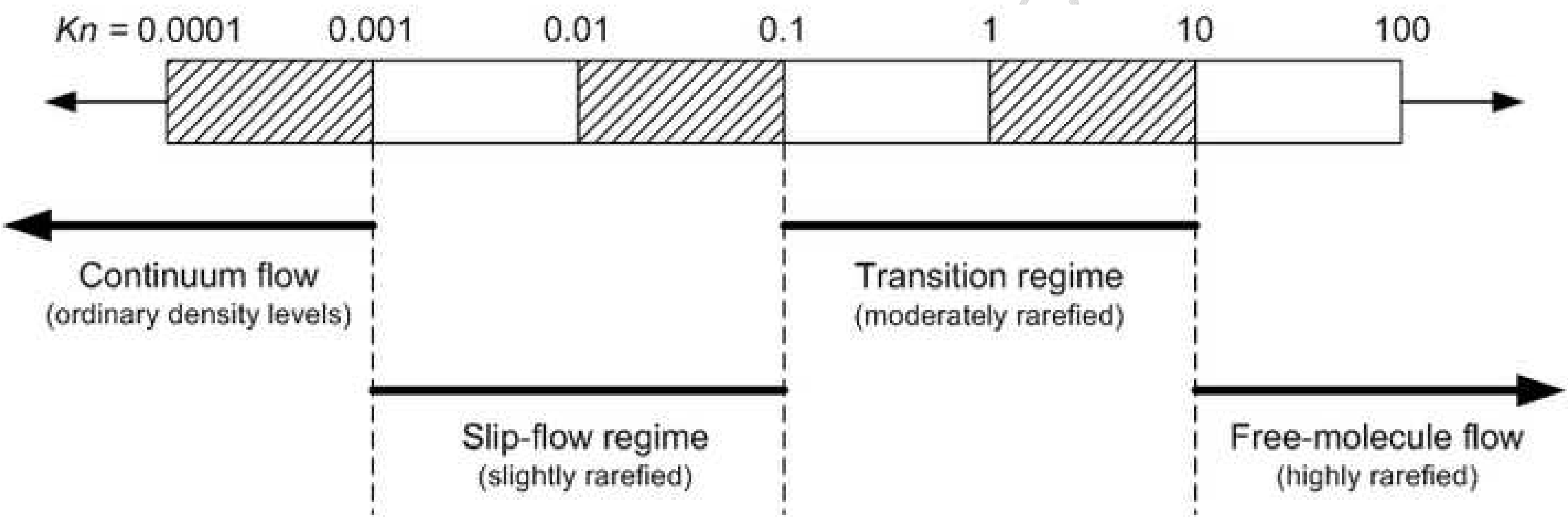
Kn = 0.0001
0.001
0.01
0.1
1
10
100
Continuum flow
(ordinary density levels)
Transition regime
(moderately rarefied)
Slip-flow regime
(slightly rarefied)
Free-molecule flow
(highly rarefied)

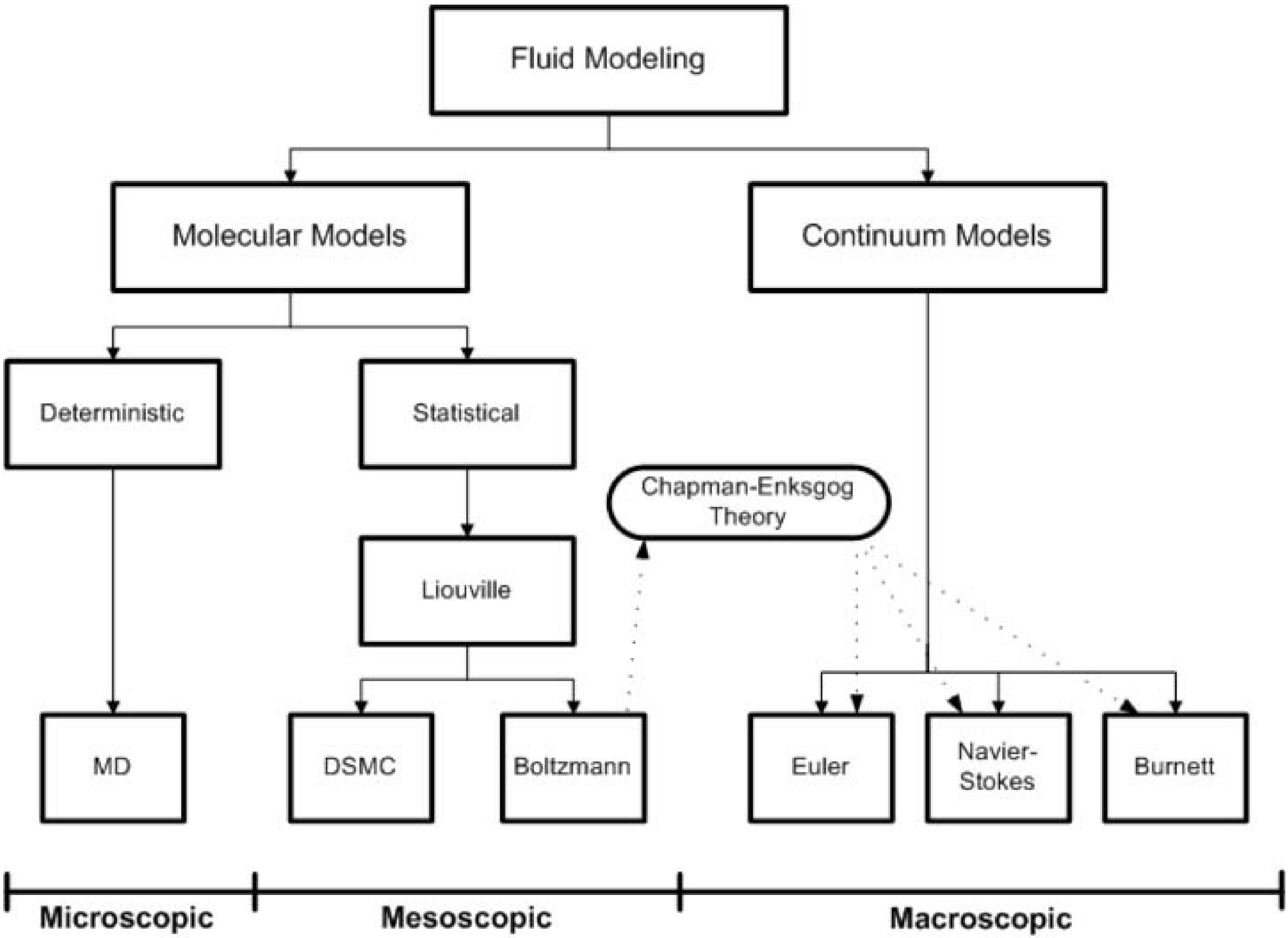
Fluid Modeling
Molecular Models
Continuum Models
Deterministic
Statistical
Chapman-Enksgog Theory
Liouville
MD
DSMC
Boltzmann
Euler
Navier-Stokes
Burnett
Microscopic
Mesoscopic
Macroscopic